國 立 交 通 大 學

生 物 科 技 學 院

生 物 科 技 學 系

碩 士 論 文

建構一以奈米金球為基礎的光學生物感測平台用於
蛋白質酶活性之檢測

Establishing a Gold Nanoparticles-Based Optical Biosensing Platform for the Assay of Proteinase Activity

研 究 生：李榕均

指導教授：林志生 博士

中 華 民 國 九 十 八 年 七 月

建構一以奈米金球為基礎的光學生物感測平台用於蛋白質酶活性之檢測

Establishing a gold nanoparticles-based optical biosensing platform for the assay of proteinase activity

研 究 生：李榕均　　Student：Jung-Chun Li

指導教授：林志生　　Advisor：Chih-Sheng Lin

國 立 交 通 大 學

生 物 科 技 學 院

生 物 科 技 學 系

碩 士 論 文

A Thesis

Submitted to Department of Biological Science and Technology

College of Biological Science and Technology

National Chiao Tung University

In partial Fulfillment of the Requirements

For the Degree of Master

In

Biological Science and Technology

July 2009

Hsinchu, Taiwan, Republic of China

中 華 民 國 九 十 八 年 七 月

建構一以奈米金球為基礎的光學生物感測平台用於蛋白質酶活性之檢測

研究生：李榕均　　指導教授：林志生 博士

國 立 交 通 大 學

生 物 科 技 學 院

生 物 科 技 學 系

摘　要

奈米金球（gold nanoparticles, AuNPs）具有獨特的物理特性，並且在光學上具有表面電漿共振吸收（surface plasmon resonance, SPR）的現象而備受注目。由於奈米金球的吸收光譜會因大小、形狀，或表面修飾上有機分子而有所差異，因此本研究利用 AuNPs 之 SPR 特性，建構出一光學式生物感測平台用於蛋白質酶（proteinase）活性之檢測。

本研究首先將明膠（gelatin）修飾於 13 nm 的 AuNPs 上作為 proteinase 之受質，同時修飾上 6-醯基己-1-醇（6-mercapto-1-hexanol, MCH）當作誘導子。當 AuNPs 修飾上 gelatin 與 MCH 時，gelatin 所造成的空間障礙可防止金球彼此間的距離拉近，避免 AuNPs 產生聚集。因此 AuNPs/MCH-gelatin 可穩定存在於極端的檢測環境中。當 proteinase 中的胰蛋白酶（trypsin）或基質金屬蛋白質酶-2（matrix metalloproteinase-2, MMP-2）降解 AuNPs/MCH-gelatin 表面上的受質後，AuNPs 失去保護，同時 MCH 增強 AuNPs 彼此間的吸引力，AuNPs 彼此間距離逐漸靠近，因而產生聚集。AuNPs 聚集時，其 SPR 會有紅位移（red-shift）現象，並且 AuNPs 的呈色會由原先的酒紅色轉變為紫色。此外，AuNPs 之顏色變化可直接以肉眼觀察，且最大吸收波峰值（λ_{max}）可經由 UV/Vis spectroscopy 量測之。

在此以奈米金球為基礎的光學式生物感測平台中，利用 AuNPs 的吸光值比值（$A_{625\ nm}/A_{525\ nm}$）估計 proteinase 之活性，針對 trypsin 之偵測線性範圍為 5×10^{-1} 至 5×10^{2} U，偵測極限為 5×10^{-1} U；而針對 MMP-2 測得的線性範圍為 50 ng/mL 到 600 ng/mL，偵測極限為 50 ng/mL。此外利用兩種 MMP-2 抑制劑，galardin 及 ONO-4817 進行藥物篩檢方面研究。利用此奈米金球系統針對 galardin 及 ONO-48 進行檢測，其 IC_{50} 值分別為 1.87 nM 以及 17.76 nM，而以酶譜分析法（zymography）所測得之 IC_{50} 值分別為 3.48 與 14.33 nM，結果顯示此兩種方式所測得之結果有高度一致性。然而此光學式生物感測系統可將偵測時間縮短到 30 分鐘內。因此，此快速且敏感性高的奈米金球光學生物感測平台具有相當潛力運用於 anti-MMPs 藥物篩檢及 MMPs 相關疾病診斷上。

關鍵字：奈米金球，蛋白質酶，光學式生物感測平台，基質金屬蛋白酶，明膠

Establishing a gold nanoparticles-based optical biosensing platform for the assay of proteinase activity

Graduate student: Jung-Chun Li Advisor: Chih-Sheng Lin Ph. D.

Department of Biological Science and Technology

College of Biological Science and Technology

National Chiao Tung University

Abstract

Gold nanoparticles (AuNPs) have interesting physical and optical property on surface plasmon resonance (SPR). Especially, AuNPs display different absorption spectra when the AuNPs possess different sizes, shapes, or being functionalized with chemical molecules. In this study, an optical biosensing platform was established and was based on the SPR property of AuNPs for the measurement of proteinase activity.

First, the 13 nm AuNPs was modified with gelatin as proteinase substrate and then modified with 6-mercapto-1-hexanol (MCH) as an inducer. When AuNPs was modified with gelatin and MCH (AuNPs/MCH-gelatin), the gelatin increased the steric repulsion of AuNPs, and prevented the AuNPs surfaces from coming into close contact. For this reason, the AuNPs/MCH-gelatin could disperse in solution, and exhibited a dramatic stability in strict environment. After the proteinase (trypsin or matrix metalloproteinase-2 [MMP-2]) digested the substrate on AuNPs/MCH-gelatin, the AuNPs lost shelter and MCH increased the attraction force between AuNPs. Therefore, the AuNPs were close to each other and gradually resulted in aggregation. The AuNPs aggregation could be monitored by a red-shift in surface plasmon absorption and color would change from wine-red to violet-purple.

Furthermore, the color change can be observed by naked eyes, and the maximum wavelength (λ_{max}) was measured by the UV/Vis spectroscopy.

In the AuNPs-based optical biosensing platform, the absorption ratio ($A_{625\ nm}/A_{525\ nm}$) of AuNPs was used to quantitively estimate the proteinase activity, and a linear range of trypsin detected by the AuNPs-based optical biosensing platform was from 5×10^{-1} to 5×10^{2} U and with a detection limit of 5×10^{-1} U. A linear correlation was established when the MMP-2 activity was from 50 ng/mL to 600 ng/mL, and with a detection limit of 50 ng/mL. Besides, two MMP-2 inhibitors, galardin and ONO-4817, were used in this study for feasibility analysis of drugs screening. In the AuNPs-based method, the MMPs activity for IC_{50} values of galardin and ONO-4817 were 1.87 nM and 17.76 nM, respectively. In comparision with zymography, MMP-2 activity for IC_{50} values of galardin and ONO-4817 were 3.48 and 14.33 nM, respectively. The result of the AuNPs-based method was consistent with that of zymography method. Furthermore, the AuNPs-based method can shorten detection time to less than 30 min. Thus, the rapid and sensitive novel AuNPs-based optical biosensing platform had potential for further applications in anti-MMPs drug screening and for MMP-related diseases diagnosis.

Keywords: Gold nanoparticles, Proteinase, Optical biosensing platform, Matrix metalloproteinase, Gelatin

誌　謝

兩年的碩士生涯，即將隨著此頁落幕，接著邁向人生新的里程碑。其實沒想過最後的學生生涯會在交大渡過，從一開始考程的排定，選錯考科，到備取備上，一波多折的過程，我想，是命中註定該到此地渡過這兩年的時光吧！

首先感謝我的指導教授林志生老師收留我這個備取生，在我研究所期間以自身嚴謹的態度來教導學生，在我學習過程中的諄諄教誨，使我在研究所期間獲益良多，在此獻上最誠摯的感謝。此外也感謝顏聰榮教授、楊昀良教授、蘇平貴教授、溫曉薇教授及吳啟華教授，謝謝各位老師撥冗來參加我的碩士學位口試，給予學生寶貴的建議，使得這本論文能更臻完善。

感謝已有幸福家庭的建龍學長、好好先生俊旭學長、雖已畢業但還是很常見面的宜貞學姐；帶領 Biosensor 組獲得不少獎項的思豪學長、提供住所讓大家吃火鍋的棠青學長、總是在電話中吵架的筱晶學姐、常被我問問題的聖壹學長、欲研發棗子芭的曜禎學長；同為宅大三人組愛摸人一把的千雅同學、暫當助理的証皓同學、藻類扛霸子之一的明達同學；碩一正妹群：庭妤、郡誼、子慧和瀞韓學妹；每次聚會出遊都會跟到的唯婷學妹與修兆學弟；從 SPCE 世界開始陪伴的欣儒學妹。感謝你們在這兩年間於實驗上及生活中各事務的幫助，使我的研究生活變得絢麗多彩，謝謝你們。

感謝隔壁實驗室與我稱兄道弟的雯雯阿布兄，很妙的認識過程，謝謝妳於兩年中跟我一起練瘋話，希望往後彼此一路順遂；好友佳穎、舞喵、乙禾老大，跟我一起環島的水餃王振暉，衷心謝謝妳們包容愛亂跳 tone 的我，並感謝你們曾在我低潮難過時陪伴我渡過。

最後，僅以此論文獻給我最親愛的家人，我的母親跟我的阿姨，謝謝你們的支持，使我得以完成我的碩士學位，願與你們分享這份榮耀！

李榕均　　謹誌

國立交通大學 生物科技學系碩士班

中華民國九十八年七月

Content

List of Tables

List of Figures

I. Literature Review

1-1 Biosensors

Since the glucose sensor was reported by Clark and Lyons in 1962 [Clark and Lyons, 1962], which generally recognized as the first biosensor, many types of biosensor and their associated techniques have been studied and developed [Bergveld, 1996; Nakamura and Karube, 2003]. According to the definition of the International Union of Pure and Applied Chemistry (IUPAC), the biosensor is the device that uses specific biological components detect of an analytic with a physicochemical detector component. Biosensors are useful tools for investigation of bio-molecular interactions [Boozer et al., 2004; Campbell et al., 2004; Bollmann et al., 2005; Buchmueller et al., 2005]. The interaction between the analyte and the biological component is designed to produce a physicochemical signal that can be measured by the transducer and can be converted into a measurable effect such as an electrical signal [Vo-Dinh and Cullum, 2000]. **Figure 1-1** illustrates the conceptual principle of the biosensing process.

1-1-1 Analytical devices

The biosensor analytical devices combine a biological material (e.g., tissue, microorganisms, organelles, cell, cell receptors, enzymes, antibodies, nucleic acids, etc.) [Cosnier et al., 2004; Davidson et al., 2004; Davis et al., 2005], intimately associated with or integrated within a physicochemical transducer which could be optical, electrochemical, thermometric, piezoelectric, magnetic or micromechanical, and that is primarily responsible for the display of the results in a user-friendly way [Cavalcanti et al., 2008].

1-1-2 Transducer

The transducer and the detector element play an important role in the detection process. Depending upon the variety form of signal resulting from the interaction between the analyte and the biological element, the transducer can be classified into electrochemical, optical, piezoelectric, thermal, etc. (**Table 1-1**). Furthermore, novel types of transducers are constantly being developed for use in biosensors. The signal can be transformed into another signal that can be more easily measured and quantified. For a given analyte-recognition element reaction, several transduction schemes may be applicable. However, constraints may be imposed by the intended use [Feriotto et al., 2004; Fojta et al., 2004; Fu et al., 2005]. A transducer should be not only highly specific for the analyte of interest, it should be able to respond in the appropriate concentration range and have a moderately rapid response time. The transducer also should be reliable, able to be miniaturized, and suitably designed for practical application [Foulds and Lowe, 1985; Alocilja and Muhammad-Tahir, 2008].

1-1-3 Bio-recognition element

Biosensors consist of bio-recognition system, typically enzymes or binding proteins, such as antibodies, immobilized onto the surface of physico-chemical transducers. Immuno-sensors are often used to describe biosensors which use antibodies as their bio-recognition system [Graham et al., 2004; Gronewold et al., 2005; Halder et al., 2005].

In addition to enzymes and antibodies, the bio-recognition system can also include nucleic acid, bacteria, single cell organisms, and even whole tissues of higher organisms. Specific interactions between the target analyte and the complementary bio-recognition layer produce a physico-chemical change which is detected and may be measured by the transducer

[Knight, 2004; Krieg et al., 2004; Ladd et al., 2004]. In principle, any bio-molecule or molecular assembly that has the capability of recognizing the analyte can be used as a bio-receptor.

1-1-4 Applications of biosensors

Biosensors are used in increasingly broader ranges of application. The following describes some of the current applications, clinical diagnosis and biomedicine, farm and veterinary analysis, process control (fermentation control and analysis), food and drink production analysis, microbiology (bacterial and viral analysis), pharmaceutical and drug analysis, industrial effluent control, pollution control and monitoring, mining and toxic gases, and military applications. The applications of biosensors are listed in **Table 1-2.**

Biosensors are beginning to move from the proof-of-concept stage to field testing and commercialization in the United States, Europe, and Japan. Biosensors have several characteristic properties. The following section describes properties of biosensors [Cho et al., 2004; Li et al., 2005].

1-1-5 Properties of biosensors

Specificity: Like other bio-analytical methods (such as immuno-assays and enzyme assays), biosensors use a biologically derived compound as the sensing element. The advantage of biological sensing elements is their remarkable ability to distinguish between the analyte of interest and similar substances. With biosensors, it is possible to measure specific analytes with great accuracy.

Speed: One characteristic of biosensors that distinguishes them from other bio-analytical methods is that the analyte tracers or catalytic products can be directly and instantaneously

measured. There is no need to wait for results from lengthy procedures carried out in centralized laboratories.

Simplicity: The uniqueness of a biosensor is that the receptor and transducer are integrated into one single sensor. This combination enables the measurement of target analytes without using reagents. For example, the glucose concentration in a blood sample can be measured directly by a biosensor (which is made specifically for glucose measurement) by simply dipping the sensor in the sample. This is in contrast to the conventional assay in which many steps are used and each step may require a reagent to treat the sample.

Continuous monitoring capability: Another advantage of biosensors is that the bio-analytical assays can regenerate and reuse the immobilized biological recognition element. For enzyme-based biosensors, an immobilized enzyme can be used for repeated assays. This feature allows these devices to be used for continuous or multiple assays. By contrast, immunoassays, including enzyme-linked immunosorbent assay (ELISA), are typically based on irreversible binding and are thus used only once and discarded.

1-2 Gold nanoparticles

Nanoparticles, especially gold nanoparticles (AuNPs), have received great interests due to their attractive electronic, unique optical, thermal and physical properties as well as catalytic properties and potential applications in the fields of bio-nanotechnology (such as drug and gene delivery, and bioimaging) and in the rapidly developing area of biosensors [Park et al., 2002; Guo and Wang, 2007; Wang et al., 2008]. Therefore, the synthesis and characterization of AuNPs have attracted considerable attention. Furthermore, they have been proposed as future building blocks in nanotechnology [Persoons and Verbiest, 2006;

Zhao et al., 2008]. **Table 1-3** shows the application of AuNPs.

Since the first synthesis report of AuNPs appeared about 150 years ago, numerous preparative methods leading to monodisperse particles of adjustable size and shape have surfaced. The common method for synthesis of AuNPs is wet chemical synthesis. Another method for the experimental generation of AuNPs is by sonolysis. The details of synthesis methods, characteristic, and application of AuNPs are as below:

1-2-1 Wet chemical synthesis techniques for small spherical particles

The common method for synthesis of AuNPs is wet chemical synthesis. In a typical synthesis of AuNPs, gold salts such as $AuCl_3$ are reduced by the addition of a reducing agent which leads to the nucleation of Au ions to nanoparticles. Furthermore, a stabilizing agent is also required for stabilize the AuNPs. The size and shape of nanoparticles greatly influences their properties [Rao and Cheethama, 2001]. For example, spherical AuNPs exhibit a single plasmon resonance in the visible region of the spectrum, while rodlike particles exhibit a longitudinal and transversal plasmon resonance [Hutter and Fendler, 2002]. The common wet chemical synthesis methods of AuNPs including the citrate reduction method and the Brust method.

The citrate reduction method: The citrate reduction method was proposed by Turkevich in 1951 and this is the most well-known and simplest method for synthesizing gold colloids. This method is used to produce modestly monodisperse spherical AuNPs involving the reduction of $HAuCl_4$ by sodium citrate in water. A typical standard citrate reduction procedure to fabricate AuNPs with an average diameter of 20 nm is as follows [Frens 1973; Grabor et al., 1997; Glomm, 2005; Persoons and Verbiest, 2006]:

Firstly, a solution of 100 mL 1 mM hydrogen tetrachloroaurate ($HAuCl_4$) in water was

boiled in reflux conditions under vigorous stirring and secondly 10 mL of 38.8 mM aqueous sodium citrate was quickly added to the $HAuCl_4$ solution. This reaction resulted in color changes of the originally yellow solution to dark blue/grey. After 2 min, the color of solution became wine-red, indicating the end of the reaction. This mixture was further stirred and boiled for 15 min and subsequently cooled to room temperature while stirring continuously. The resulted colloidal AuNPs are approximately spherical and have an overall negative surface charge due to the citrate coverage. In the reaction, the citrate ions reduce the gold salt $HAuCl_4$ according to

$$3\,(H_2CCOOH)_2C(OH)COO^- + 2AuCl^-_4 \leftrightarrow$$
$$3\,(H_2CCOOH)_2C{=}O + 2Au + 8Cl^- + 3CO_2 + 3H^+$$

The gold colloids are stabilized by negatively charged citrate ions and chloride ions that are still present in the solution. The citrate is not only as a reductant but also as a kinetic stabilizer. Irreversible aggregation or coagulation is easily induced by addition of electrolytes (e.g. KI, NaCl, and KNO_3) to the solution. The AuNPs size can be control by changing the concentration of the added sodium citrate [Frens, 1973]. To synthesis larger particles, less sodium citrate should be added. However, the results are less reproducible, the larger particles are less monodisperse and the color of the solution is violet, indicating the importance of the citrate ions stabilizing the gold colloids [Glomm, 2005; Persoons and Verbiest, 2006]. The AuNPs are stabilized by electrostatic repulsion due to adsorbed citrate ions on their surface that impart negative charge to the nanoparticles [Turkevich, 1985; Nath and Chilkoti, 2004].

The Brust method: This two-phase synthesis method was described by Brust and Schiffrin in 1994, and can be used to synthesize AuNPs in organic liquids that are normally not miscible with water [Brust et al., 1994].

In the Brust method, the gold colloids are sterically stabilized by organic molecules

having thiol, amide or acid groups in the solutions. The stabilization with organic molecules having thiols is due to the covalent bond that gold binds specifically to the sulfur atom of the thiol group [Rodriguez et al., 2003] while the organic molecules forms the actual stabilization preventing the particles to aggregate. The main advantage of the Brust method is that the AuNPs behaves like chemical compounds [Whyman, 1996]. The AuNPs can be precipitated, filtered off and redissolved in organic solutions. Furthermore, several stabilization agents with thiol, amide or acid groups can be used to sterically stabilize the gold colloids. The preparation processes is as follows [Brust et al., 1994]:

First, 30 mL of a 30 mM aqueous solution of $HAuCl_4$ was mixed with a solution of tetraoctylammonium bromide (TOAB or TOABr) in 80 mL 50 mM toluene ($C_6H_5CH_3$) and stirred vigorously. After the tetrachloroaurate was transferred into the organic layer, the l70 mg dodecanethiol was then added to the organic phase. Second, 25 mL of a freshly prepared 0.4 M aqueous solution of sodium borohydride ($NaBH_4$) was slowly added with vigorous stirring. After further stirring for 3 hr the organic phase was separated, and evaporated to 10 mL in a rotary evaporator. To remove the excess of thiocholesterol, the organic phase was mixed with 400 mL ethanol. The mixture is then kept at -18°C for 4 hr and the dark brown precipitate was filtered off and washed with ethanol. The crude product was dissolved in 10 ml toluene and again precipitated with 400 ml ethanol. The overall reaction is as follows [Brust, 1994]:

$$AuCl_4^- (aq) + N(C_8H_{17})_4^+ (toluene) \rightarrow N(C_8H_{17})_4^+ AuCl_4^- (toluene)$$

$$mAuCl_4^- (toluene) + nC_{27}H_{45}SH (toluene) + 3me^- \rightarrow$$

$$4mCl^- (aq) + (Aum) (C_{27}H_{45}SH)n (toluene)$$

1-2-2 Synthesis of AuNPs by ultrasound

An alternative method for the fabrication of AuNPs is by ultrasound method. This

method can effectively form gold complexes and only after the addition of a suitable reducing agent to the sonicated solution will the formation of AuNPs be observed. The mechanism of the fabrication of the AuNPs depends on the pyrolysis of water and other organic compounds present in the aqueous solution resulting in the formation of free radicals at high temperatures and pressures. When water is sonicated in the presence of ethanol, the following reactions proceed [Okitsu et al., 2001; Caruso et al., 2002]:

$$H_2O \rightarrow \bullet H + \bullet OH$$

$$CH_3CH_2OH + \bullet H(\bullet OH) \rightarrow CH_3CH\bullet OH + H_2\ (H_2O)$$

$$CH_3CH_2OH \rightarrow \text{pyrolysis radicals}$$

These radicals can reduce gold(III) ions into gold(II), gold(I), and finally gold(0). When the $AuCl_4^-$ is sonicated in water without the addition of ethanol, some AuNPs is produced according to three separate near diffusion-controlled one-electron transfer steps with H• as the primary reducing species [Caruso et al, 2002]:

$$AuCl^-_4 + 3H\bullet \rightarrow Au(0) + 4Cl^- + 3H^+$$

And in the presence of ethanol a more complex sequence of three separate one-electron transfer reactions may be summarized [Okitsu et al, 2001; Caruso et al, 2002]:

$$3CH_3CH\bullet OH + AuCl_4^- \rightarrow 3CH_3CHO + Au(0) + 4Cl^- + 3H^+$$

The reduction of $AuCl_4^-$ to colloidal gold according to the above two reactions is simplified and the particle growth is much more complex in the real sample solution. The rate of gold(III) reduction can be controlled by the ultrasound irradiation conditions such as the temperature and the ultrasound intensity. The size of the AuNPs can be controlled by changing the alcohol concentration and alkyl chain length [Caruso et al, 2002]. This method is useful in the rapid fabrication of AuNPs, but the particles are polydisperse which is a problem for applications where monodisperse solutions are required [Persoons and Verbiest, 2006].

1-2-3 Synthesis process of AuNPs

The synthesis process of AuNPs involves three distinct stages: nucleation, growth and coagulation [Turkevich, 1985; Goia and Matijevic, 1998; Goia and Matijevic, 1999].

In the first stage, nucleation, metal ions are reduced to metal atoms, and rapid collisions to form stable icosahedral nuclei of 1-2 nm in size. The factors that affect the initial concentration of nuclei include the following: the concentration of the reducing agent, the solvent, temperature and reduction potential of the reaction. Increasing the molar ratio of reducing agent to metal salt causes rapid formation of a large number of nuclei and leads to smaller, monodisperse AuNPs. In contrast, decreasing the molar ratio leads to slow formation of a few nuclei, and results in larger AuNPs with a greater heterogeneity in size. This stage is important for controling the shape, size and structure distribution of AuNPs and is typically complete in a few seconds. In the growth stage, the metal ions are reduced on the surface of the nuclei, until all the metal ions are consumed. The final stage for synthesis of AuNPs is coagulation, which involves prevention of AuNPs aggregation by the addition of stabilizing agents, which is either adsorbed or chemically bound to the surface of the AuNPs, and is typically charged. The equally charged AuNPs repel each other so that they are colloidally stable [Sperling et al., 2008].

1-3 Surface modification and bioconjugation of AuNPs

AuNPs are surrounded by a shell of stabilizing molecules. One end of these stabilizing molecules are either adsorbed or chemically linked to the gold surface, while the other end points towards the solution and provides colloidal stability [Sperling et al., 2008]. After synthesis of AuNPs, the stabilizer molecules can be replaced by other stabilizer molecules in a

ligand exchange reaction [Pellegrino et al., 2005].

Biological molecules can be attached to the AuNPs in several ways. If the biological molecules have a functional group which can bind to the gold surface (e.g., -SH, -CN, -NH_2, -COOH, -OH), the biological molecules can replace some of the original stabilizer molecules when they are added directly to the AuNPs solution [Grabar et al., 1995; Kumar et al., 2004; Sperling et al., 2008]. By choosing the suitable molecules, it is possible to adjust the surface properties of the particles and attach different kinds of molecules to the AuNPs.

1-4 Surface plasmon resonance of AuNPs

AuNPs have emerged as important colorimetric reporters because of their high extinction coefficients and strongly distance-dependent optical properties [Kim et al., 2001; Huang et al., 2005], the interesting optical and electronic properties that have served as a versatile platform for exploring many facets of basic science. AuNPs can strongly absorb and scatter visible light. When visible light shines on AuNPs, the light of a resonant wavelength is absorbed by AuNPs and the visible light energy excites the free electrons in the AuNPs. The phenomenon induces surface electron oscillation of AuNPs and is responsible for the intense colors exhibited of AuNPs, the so-called surface plasmon resonance (SPR) [Sönnichsen et al., 2002; Nath and Chilkoti, 2004; Sperling et al., 2008; Zhao et al., 2008]. The schematic presentation of the SPR is shown in **Figure 1-2**. And the SPR depends strongly on the size, shape, medium, and the relative distance of the AuNPs [Su et al., 2003; Sun and Xia, 2003; Schultz, 2003]. The **Figure 1-3** shows UV-Vis absorption spectra of AuNPs with different diameters.

Small AuNPs (e.g., 13 nm in diameter) absorb green light, which corresponds to a strong

absorption band (surface plasmon band) at about 520 nm in the visible light spectrum, resulting in the AuNPs display red in color. When the AuNPs are small, the surface electrons are oscillated by the incoming light in a dipole mode. As the size of AuNPs increases, the light can no longer polarize the nanoparticles homogeneously. Hence, the higher order modes at lower energy dominate. This causes a red-shift and broadening of the surface plasmon resonances. Therefore, the surface plasmon band red shifts with increasing AuNPs size [Ghosh and Pal, 2007; Zhao et al., 2008]. The red shift and color change also can be observed during the aggregation of small AuNPs. The spherical AuNPs with interparticle distance higher than the average particle diameter appear red in color. When the interparticle distance become smaller than the average particle diameter, their surface plasmons combine (interparticle plasmon coupling), and the aggregate could be considered as a single large particle, resulting in color changes from red to blue [Link and El-Sayed, 1999; Jena and Raj, 2008; Zhao et al., 2008]. The interparticle plasmon coupling can generate a huge absorption band shift (up to ~300 nm), and the color change can be observed by the naked eye. Therefore, complicated instruments are not required for analysis.

This unique optical property of AuNps can provide an elegant colorimetric platform for detection biological molecular interaction. When target analyte or a biological molecular which directly or indirectly triggers AuNPs aggregation (or redispersion of an aggregate), this process can be detected by the color change of the AuNP solution. The ratio of the absorbances at 520 nm (for 13 nm AuNPs), which corresponds to dispersed particles, and a longer wavelength (e.g., 600 nm), which corresponds to aggregated particles, is often used to quantify the aggregation process or color change [Zhao et al., 2008].

1-5 Nanoparticles stability - DLVO theory

DLVO theory was developed by Derjaguin, Landau, Verwey and Overbeek in the 1940s, and has been used to explain the stability of colloids in suspension. The theory describes the force between charged surfaces interacting through a liquid medium. The stability of colloidal system is determined by the balance between two opposing forces: electrostatic repulsion and van der Waals attraction [Craig et al., 1998; Malvern Instruments]. The particle interaction forces are described by **Figure 1-4**.

The dominant cause of aggregation is the van der Waals attractive forces between the particles, which are long-range forces [Shaw, 1980]. Van der Waals attraction is actually the result of attractive forces acting between individual particles in colloid system. The effect is accumulative. One particle of the first colloid has a van der Waals attraction to each particle in the second colloid. This phenomenon is repeated for each particle in the first colloid, and the sum of all of these is the total attractive forces. The variation in van der Waals force with distance between the particles is demonstrated by an attractive energy curve [Zeta-Meter, Inc. 1993; Pashley and Karaman, 2005].

The DLVO theory proposes that an energy barrier resulting from the repulsive force prevents particles aggregation. The particles will suspension in the solution, and the system will be stable. However, if the particles collide with sufficient energy to overcome that barrier, the attractive force will pull them approaching and adhering each other, the particles will be irreversibly aggregation. An electrostatic repulsion curve is used to indicate the energy that must be overcome if the particles are to be forced together. The maximum energy is related to the surface potential and the zeta potential. Therefore, the repulsive forces plays an important role in maintain the stability of the colloidal system. There are two essential mechanisms that affect dispersion stability.

Steric repulsion: The stability of colloidal dispersions can be enhanced by the addition of suitable material (protective agents) adsorbing or otherwise attaching to the particle surfaces and preventing the particle surfaces coming into close contact [Shaw, 1980; Persoons and Verbiest, 2006]. If enough material adsorbs to the particles, the coating is sufficient to keep particles separated by steric repulsions between the polymer layers, and the van der Waals forces are too weak to cause the particles to aggregate. The mechanism of steric stabilization is simple, requiring just the addition of a suitable material. However, the material can be expensive and in some cases the material is undesirable for subsequently aggregate the system if that is required [Malvern Instruments].

Electrostatic or charge stabilization: The effect on particle interaction results from the distribution of charged species in the colloid system. Energy is required to overcome this repulsion. An electrostatic repulsion curve is used to indicate the energy that must be overcome if the particles are to be forced together. The maximum energy is related to the surface potential and the zeta potential. This mechanism can stabilize or aggregate the particles in the system by altering the concentration of ions in the surrounding. This process is simple and potentially inexpensive [Zeta-Meter, Inc. 1993; Pashley and Karaman, 2005; Malvern Instruments].

1-6 Applications of AuNPs

1-6-1 Applications of AuNPs in biosensors

AuNPs have great potential applications in the field of biosensors due to their display many interesting electrical and optical properties. AuNPs can exhibit surface plasmon resonance and plasmon absorption in the red-shift due to interparticle plasmon interactions

[Wang et al., 2009]. This optical property of AuNPs can establish a highly selective and sensitive colorimetric assays for molecular recognition events [Rosi and Mirkin, 2005; Jena and Raj, 2008]. AuNPs-based colorimetric assays for detection are mainly dependent on the analyte induce the change of interparticle distance of AuNPs, and resulting in color change of AuNPs. Since the first AuNPs-based DNA sensor was developed by Mirkin and coworkers [Mirkin et al., 1996], the AuNPs-based platform has been increasingly applied for the detection of a large variety of targets, including nucleic acids [Cao et al., 2005; Li et al., 2005; Chen et al., 2008], proteins [Tsai et al., 2005; Chen et al., 2008], enzyme activity [Xu et al., 2007; Jiang et al., 2009] and metal ions [Liu and Lu, 2007; Slocik et al., 2008].

Besides, the exceptional quenching ability of AuNPs makes them excellent materials for Förster resonance energy transfer (fluorescence resonance energy transfer; FRET)-based biosensors [Sapsford et al., 2006; De et al., 2008]. The fluorescence of many fluorophores is quenched when they are in close proximity to AuNPs surface [Dulkeith et al., 2002; Sperling et al., 2008]. For detection of analyte, AuNPs are conjugated with ligands that specifically bind to the analyte, and analyte molecules are modified with fluorophores. When the analyte and ligand have interaction, the fluorophores are closely linked to the AuNPs and their fluorescence is quenched. Another detection scheme works slightly differently. In this case a molecule is used as a spacer to link fluorophores to AuNPs. In the presence of the analyte, the spacer molecule changes its conformation, resulting in quenching or releases the fluorescence of the fluorophore [Sperling et al., 2008]. The FRET-based biosensors has been used for the detection of nucleic acids [Maxwell et al., 2002; Ray et al., 2006] and proteins [Oh et al., 2005; Oh et al., 2006; Huang et al.,2007].

Finally, AuNPs can also be used for the transfer of electrons in redox reactions, due to their conductivity and catalytic property [De et al., 2008; Sperling et al., 2008]. In the electrochemical biosensor, enzyme can specifically oxidize (or reduce) the analyte molecules,

and the flow of electrons released (or required) in this redox reaction can be measured as electrical current. Therefore, enzyme is conjugated with the AuNPs [Xiao et al., 2003], and immobilized on the surface of an electrode which is connected to an amplifier for current detection. Alternatively, AuNPs also can be first immobilized on the electrode and then modified with enzymes [Xiao et al., 1999]. The electrode covered with a layer of AuNPs has a larger surface area, and the enzyme conjugated with the AuNPs can facilitate the electron transport, these lead to enhance the currents [Sperling et al., 2008].

1-6-2 Applications of AuNPs in drug delivery system

AuNPs have been used for a long time for drug delivery systems (DDSs). Biology molecules are adsorbed on the surface of AuNPs and introduced into the cells. The methods for particles introduction into a cell can either be forced as in the case of gene guns or achieved naturally by particles ingestion. These molecules will eventually detach themselves from the surface of the AuNPs when inside the cells [Sperling et al., 2008].

The method of gene guns is using AuNPs as massive nanobullets for ballistic projectile introduction of DNA into cells. DNA is adsorbed onto the surface of AuNPs which are then shot into the cells. This method has been used successfully for gene delivery [Tischer et al., 2002; Lee et al., 2008].

Another method for AuNPs application of drug delivery is achieved naturally by particles ingestion. As good biocompatible materials, AuNPs can be modified with bio-molecular and would not destroy their biological activity. Furthermore, AuNPs can be uptaken by cells naturally, either specifically (via receptor-ligand interaction) or nonspecifically [Chithrani et al., 2006; Sperling et al., 2008]. For specific uptake, the ligands specific to receptors on the cell membrane are conjugated to the surface of the AuNPs. In this way, ligand-modified AuNPs are predominantly incorporated by cells which possess

receptors for these ligands, and is more effective than nonspecific uptake [Sperling et al., 2008]. It is possible to direct particles specifically to cancer cells by conjugating them with biomarkers on the surface of cancer cells but that are less present on healthy cells [Jain et al., 2007]. After ingestion, the AuNPs are stored in vesicular compartments inside the cells [Chithrani and Chan, 2007]. In order to release the particles from the vesicular structures to the cytosol, their surface can be coated with membrane-disruptive peptides or relying on the acidic condition inside tumor and inflamed tissues (pH~ 6.8) and cellular compartments including endosomes (pH~ 5.5-6) and lysosomes (pH~ 4.5-5.0) [de la Fuente and Berry, 2005; Yang et al., 2005]. AuNPs uptake-mediated delivery of molecules into cells is used mainly for two applications. First, gene therapy DNA is introduced into cells, which subsequently causes the expression or down-expression of the corresponding proteins [Sullivan et al., 2003; Salem et al., 2003]. Second, targeting anti-cancer drugs are specifically delivered to cancer tissue [Rojo et al., 2004; Jain et al., 2007].

1-6-3 Applications of AuNPs in bioimaging

AuNPs have been primarily used for bioimaging, based on the interaction between AuNPs and light. AuNPs are a very attractive contrast agent as they can be visualized with a large variety of different techniques [Sperling et al., 2008].

Immunostaining is one of the traditional methods that uses AuNPs in biology. Firstly, AuNPs are conjugated with antibody for molecular recognition. The antibody-modified AuNPs will bind to the antigen or target regions containing the antigen. The antibody-modified AuNPs are added to fixed and permeabilized cells. Targets outside as well as inside cells can be labelled with AuNPs in this way. The AuNPs then provide excellent contrast for TEM imaging with high lateral resolution and larger structures can also be imaged with optical microscopy [Faulk and Taylor, 1971; De Mey et al., 1982].

AuNPs are not only used for visualizing structures within single cells, but also applied for providing contrast in vivo to whole organs in animals and potentially in humans. Firstly, the AuNPs are conjugated with antibodies or ligands which bind as specifically as possible to the organ of interest in the animal. When modified AuNPs are injected into the bloodstream of animals, these particles label at the target organs via receptor-ligand interaction [Sperling et al., 2008]. AuNPs bound to the organ provide contrast for imaging and resolving the structure of the organ. X-rays, which can penetrate skin and organs deep inside the body can be imaged or addressed for therapy [Hainfeld et al., 2004]. Furthermore, AuNPs have the predominance of causing less cytotoxic damage than quantum dots, and that makes AuNPs possess more potential to be applied in medical applications.

1-7 Matrix metalloproteinases

Matrix metalloproteinases (MMPs) are a family of extracellular zinc-dependent endopeptidases [Birkedal-Hansen et al., 1993] that are able to degrade all components of the extracellular matrix (ECM), including fibrillar and non-fibrillar collagens, gelatin, fibronectin, laminin, and basement membrane glycoproteins [Fedarko et al., 2004; Lombard et al., 2005]. MMPs not only play an important role in ECM remodeling in physiologic situations, such as embryonic development, cell migration, tissue regeneration, wound repair, apoptosis, angiogenesis, and inflammatory, but also in pathological conditions, including rheumatoid arthritis, osteoarthritis, atherosclerotic plaque rupture, tissue ulceration, and in involved in the processes of tumors metastasis and growth [Miyazaki et al., 1990; Koivunen et al., 1999; Bergers et al., 2000; Roeb and Matern, 2001; Jones et al., 2003]. The levels of MMPs can be determined in patient serum or urine, where levels elevated over a particular threshold can sometimes predict progression or prognosis (**Table 1-4**).

MMPs are generally divided into six groups, collagenases (MMP-1, -8, and MMP-13), stromelysins (MMP-3, -10 and MMP-11), matrilysins (MMP-7 and MMP-26), gelatinases (MMP-2 and MMP-9), membrane-type matrix metalloproteinases (MT-MMPs) (MMP-14, -15, -16, -17, -24 and MMP-25) and others [Jones et al., 2003]. Classification and nomenclature of all the types of MMPs were listed in **Table 1-5.** Although MMPs are subclassified based on their ability to degrade various proteins of the ECM, they also play other important roles such as the activation of cell surface receptors and chemokines [Stefanidakis and Koivunen, 2006]. In addition, MMP-2 has proteolytic activity to specific targets within the cell to cause acute, reversible contractile dysfunction in cardiac disease [Schulz, 2007].

The regulation of MMPs occurs at many levels, including transcription (the major one), post- transcriptional modulation of mRNA stability, secretion, localization, zymogen (proenzyme) activation and inhibition of activity by natural inhibitors of MMPs, tissue inhibitor of metalloproteinases (TIMPs). The TIMP gene family consists of 4 members: TIMP-1, -2, -3 and -4. TIMPs inhibit the activity of MMPs by binding to activated MMPs in a 1:1 molar stoichiometry [Brew et al, 2000]. TIMPs can also inhibit the growth, invasion and metastasis of malignant tumours [Vihinen and Kähäri, 2002].

1-7-1 Gelatinase A (MMP-2)

In 1978, Sellers et al. were first to separate a gelatinase activity from collagenase and stromelysin in the culture medium from rabbit bone [Seller et al., 1978]. Similar enzyme acting on basement membrane type IV collagen was reported by Liotta et al. [Liotta et al., 1979] in the following year. Gelatinase was purified from human skin, mouse tumor cells, rabbit bone, and human gingival. Gelatinase A was a triple repeat of fibronectin type I domains inserted in the catalytic domain; this domain participates in binding to the gelatin

substrates of the enzyme [Libson et al., 1995; Lee et al., 1997]. MMP-2 is ubiquitously expressed in the cells which comprise the heart and is found in normal cardiomyocytes, as well as in endothelium, vascular smooth muscle cells and fibroblasts [Coker et al., 1999]. In particular, MMP-2 is overexpressed in many cancers, including breast cancers, and is an indicator of cancer invasiveness, metastasis, angiogenesis, and treatment efficacy [Ratnikov et al., 2002].

1-8 Activation of MMPs

The MMPs are produced as zymogens. The basic structure of MMPs can be divided into three structural well-preserved domain motifs, including a catalytic domain, an N-terminal domain and C-terminal domain. Zinc-dependent catalytic domain (about 170 amino acids) of MMPs contains a zinc binding motif HEXXHXXGXXH as the zinc binding active site, and having an additional structural zinc ion and 2-3 calcium ions, which are required for the stability and the expression of enzymic activity [Nagase and Woessner,1999; Jones et al., 2003]. The N-terminal domain (propeptide domain; about 80 amino acids) contains a unique PRCG(V/N)PD sequence in which the cysteine residue interacts with the catalytic zinc atom in the active site, prohibiting activity of the MMPs. Thus, the interaction has to be disrupted to “open” the cysteine switch in the process of MMPs activation [Van Wart and Birkedal-Hansen, 1990], which is a critical step that leads to ECM breakdown [Carmli et al., 2004]. The C-terminal hemopexin domain (about 210 amino acids) of MMPs has a four-bladed propeller structures and contributes to substrate specificity [Wallon and Overall, 1997]. In membrane-type MMPs, the hemopexin domain contains a transmembrane domain for anchoring the protein in the membrane. Besides, the hemopexin domain in MMP-2 also has a function in the activation of the enzyme [Morgunova et al.,

1999].

All MMPs are synthesized in the latent form and require extracellular activation. MMPs can be activated *in vitro* by a variety of mechanisms. Activation of latent MMPs is believed to occur by dissociation of the sulfhydryl group of the cysteine from the active zinc site and replacement with a water molecule that plays a role in catalysis [Van Wart and Birkedal-Hansen, 1990; Galazka et al., 1996]. Disruption of the Cys-zinc bond can be achieved by heavy metal ions, oxidants, organomercurials, sulfhydryl alkylating agents, or disulfide compounds [Murphy et al., 1980; Macartney and Tschesche, 1983; Weiss er al., 1985; Stricklin et al., 1983; Mallya and Van Wart., 1989]. Latent MMPs can also be activated by conformational changes of the polypeptide chain induced by detergents or chaotropic agents [Birkedal-Hansen and Taylor, 1982; Springman et al., 1990], and also by limited cleavage of the propeptide by proteolytic enzymes such as trypsin or chymotrypsin [Murphy et al., 1980; Stricklin et al., 1983; Okada et al., 1990].

1-9 Substrate zymography

Zymography and reverse zymography are described as sensitive, quantifiable, and functional assay to detect MMPs and TIMPs in biological samples [Leber and Balkwill, 1997; Hawkes et al., 2001]. All types of substrate zymography derive from gelatin zymography. The techniques are the same except that the substrate differs depending on the type of MMPs or TIMPs to be detected. The standard method is based on sodium dodecyl sulfate (SDS) polyacrylamide gels impregnated with a protein substrate, and proteins are separated by electrophoresis under denaturing conditions [Leber and Balkwill, 1997; Snoek-van Beurden and Von den Hoff, 2005].

After electrophoresis, the gel is washed, and exchange of the SDS with Triton X-100, which cause the enzymes partially renature and recover their activity. Additionally, the latent MMPs are autoactivated without cleavage. During incubation, the renatured MMPs in the gel will digest the substrate. After incubation, the gel is stained with Coomassie Blue, and the MMPs are detected as clear bands against a dark blue background of undegraded substrate. The clear bands in the gel can be quantified by densitometry [Heussen and Dowdle, 1980; Woessner, 1995; Hawkes et al., 2001]. Zymography is based on the following principles: First, during electrophoresis, gelatin is retained in the gel. Second, MMPs activity can be reversibly inhibited by SDS during electrophoresis. Finally, the SDS causes the separation of MMP-TIMP complexes during electrophoresis. This enables the detection of MMPs and TIMPs independently of one another [Leber and Balkwill, 1997; Hawkes et al., 2001].

A particular advantage of zymography is that both the proenzymes and the active forms of MMPs can be distinguished on the basis of their molecular weight. The inactive proenzyme is about 10 kDa larger than the activated form. An additional advantage of zymography is that during electrophoresis the TIMPs dissociate from the MMPs, and do not interfere with detection of the enzymatic activity, which is not possible in solution assays [Woessner JF Jr. 1995; Leber and Balkwill, 1997]. However, there are many problems with the zymography. First, the limited number of wells per gel does not allow a full standard curve and several samples to be run on the same gel. Second, the refolding of MMPs after electrophoresis recovers only part of the original activity. Third, the two-step staining/destaining method is not reliable and is difficult to reproduce. Traditionally, the destaining step is undefined length, usually several hours until a satisfactory background/band staining is achieved. Furthermore, overstaining of the gels reduces the assay sensitivity, because bands of low activity will become undetectable. In addition, excess destaining can

also bleach the bands, so that the intensity of gels cannot be assessed in the linear range of the assay [Leber and Balkwill, 1997; Snoek-van Beurden and Von den Hoff, 2005].

II. Research Strategy

Traditional methods for analyzing the activity of MMPs include the zymography and fluorescein-labeled synthetic peptides [Leber and Balkwill, 1997; Netzel-Arnett et al., 1991]. The zymography is time consuming and complicated for MMPs activity and inhibition studies. Moreover, fluorescein-labeled synthetic peptides increase the cost of diagnosis and need expensive instruments to operate and analyze. Therefore, the SPR property of AuNPs is used to establish an AuNPs-based optical biosensing platform for measuring proteinase activity and screening the inhibitors of proteinase.

Most of AuNPs-based diagnoses for the detection of enzyme activity mainly depend on the enzyme properties to induce the change in AuNPs aggregation [Wang et al., 2006; Xu et al., 2007]. However, using AuNPs to establish a platform for detection of enzyme activity may encounter the following problems. First, ion concentration effects enzyme activity and AuNPs aggregation. When enzymes carry out their function, changing in the niche (such as pH, temperature, metal ion, or salt concentration) would affect the activity of enzymes; therefore the diagnostic system should provide an adequate environment for enzyme working. In terms of AuNPs, AuNPs would easily aggregate while surface charge is neutralized by counterions. In previous AuNPs-based sensing systems, AuNPs aggregation relies on electrostatic interaction, while the surface charges of receptor-modified AuNPs become neutral upon the addition of target analyte [Sato et al., 2003; Zhao et al., 2007; Chen et al., 2008]. Combining above problems, when the AuNPs-based sening system is applied to assay enzyme activity, not only the analyte would promote monodispersed AuNPs to aggregate, but also the cation which are supplied by the enzyme buffer may induce AuNPs to aggregate, it would result in false-positive results and interfere the analysis of enzyme activity.

Moreover, according to the DLVO theory, the stability of colloidal system is determined by the balance between two opposing forces - electrostatic repulsion and van der Waals attraction [Craig et al., 1998; Malvern Instruments]. When the bio-recognition element was modified onto AuNPs as the substrate, the bioelement molecule provides the steric repulsion and prevents the AuNPs coming into close contact [Glomm, 2005; Persoons and Verbiest, 2006]. In a detection of protein-protein interaction like proteinase digestion, the steric hindrance between the proteins would lead AuNPs dispersion and the slow enzyme kinetics would prolong the detection time. In addition, AuNPs have high affinity for biomolecules [Lu et al., 2007], which can conjugate with amino acids that have thiol, amino, carboxylic, or hydroxyl groups in their side chains. Therefore, the protein which was digested by proteinase would adsorb on AuNPs again and interfere with the aggregation of AuNPs.

To overcome these arduous problems, in this study, the colloidal AuNPs was modified with gelatin as proteinase substrate, and then modified with 6-mercapto-1-hexanol (MCH) not only as inducer but also for blocking of this system. **Figure 2-1** illustrates the schema of this platform and **Figure 2-2** shows the experimental flowchart of this study.

When the AuNPs was modified with gelatin, the gelatin adsorbed onto the AuNPs surface not only as proteinase substrate but also increase the steric repulsion of AuNPs which can prevent the particle surfaces coming into close contact. After proteinase digested the AuNPs/gelatin, the AuNPs/gelatin still can suspend stably in the solution and retain red-wine due to the steric repulsion generated by gelatin was too difficult to overcome. Hence, the MCH) was used in this system for solve the problem.

The chemical compound, MCH, played an important role as an inducer. The MCH has two functional groups, one side is thiol group (-SH), and another is hydroxyl group (-OH). Both functional group of MCH can conjugate with AuNPs by covalent bond and the -SH group has stronger attraction with AuNPs than -OH group. Therefore, in the modified

process, the MCH predominantly functionalized with gelatin AuNPs by SH-Au covalent bond and the -OH group was been exposed on AuNPs surface [Sato et al., 2003; Chen et al., 2008]. In addition, the MCH can remove nonspecifically adsorbed of gelatin from the AuNPs surface, which helps to improve subsequent biomolecular recognition efficiency [Zhao et al., 2008].

When the AuNPs was modified with gelatin and MCH, the AuNPs/MCH-gelatin could suspend stably. After proteinase digested gelatin, the AuNPs/MCH-gelatin lost the shelter, the repulsion of steric hindrance generation by gelatin was decreased and MCH attracted other AuNPs by OH-Au covalent bond [Zhu et al., 2008]. MCH induced the AuNPs to irreversibly aggregated and resulted in shift in the surface plasmon spectrum and a consequent color change of the AuNPs from red to purple. Besides, MCH modified on the AuNPs also plays the role as a blocker [Huang et al., 2007]. The MCH possessed the ability to bind on the surface of AuNPs where not conjugated with gelatin through the covalent bond, and prevent the gelatin which digested by proteinase to conjugate with AuNPs again.

In the system, the color change of AuNPs can be observed with the naked eye, and the maximum wavelength (λ_{max}) can be measured by UV/Vis spectroscopy. In addition, the method could serve as an alternative platform for efficient screening of the proteinase inhibitors. When the proteinase was inhibited by candidate drugs, the drugs block activity of proteinase, the AuNPs/MCH-gelatin are intact and stably in the solution without the color change. Therefore, the novel AuNPs-based optical biosensing platform can not only detect the activity of proteinase rapidly, but also can screen a great deal of effective inhibitor for proteinase.

III. Materials and Methods

3-1 Reagents and solutions

All chemicals were of analytical grade and were used without further purification. Sodium citrate ($C_6H_5Na_3O_7 \cdot 2H_2O$) was obtained from Merck (Darmstadt, Germany). Tris HCl was purchased from Chemicon (Invitrogen, San Diego, LA, USA). Sodium chloride (NaCl) was purchased from USB (Cleveland, OH, USA). Agarose and 10 X Tris-Borate-EDTA buffer (TBE) were purchased from Amresco (Cleveland, OH, USA). ONO-4817 ($C_{22}H_{28}N_2O_6$) was purchased from Tocris (Ellisville, MO, USA). Galardin (Ilomastat; GM6001; $C_{20}H_{28}N_4O_4$) was purchased from USBiological (Swampscott, MA). 40% acrylamide/Bis solution (37.5:1) was purchased from Bio-Rad (Hercules, CA, USA).

Calcium chloride ($CaCl_2$), trypsin, 6-mercapto-1-hexanol (MCH), triton X-100, dimethyl sulfoxide (DMSO), *p*-Aminophenylmercuric Acetate (APMA), type A gelatin, glycine, hydrogen tetrachloroaurate(III) ($HAuCl_4 \cdot 3H_2O$), coomassie brilliant blue R250, matrix metalloproteinase-2 human (expressed in mouse NSO cells) were obtained from Sigma-Aldrich (St. Louis, MO, USA).

Nanopure water was obtained by passing twice-distilled water through a Milli-Q system (18 MΩ· cm; Millipore, Bedford, MA, USA).

3-2 Preparation of the AuNPs/MCH-gelatin

3-2-1 Synthesis of 13 nm AuNPs

The 13 nm AuNPs was prepared by citrate reduction of $HAuCl_4 \cdot 3H_2O$ according to the

literature procedure [Saraiva and de Oliveira, 2002]. A 50 mL aqueous solution consisting of 2.5 mM $HAuCl_4 \cdot 3H_2O$ was brought to a vigorous boil with stirring in a conical flask, and then 38.8 mM sodium citrate (5 mL) was added to the solution rapidly. This solution was boiled with vigorous stirring for another 15 min, resulted in the color change from the originally yellow solution to deep red. The solution was cooled to room temperature with continuous stirring for 15 min. The colloidal AuNPs with an average diameter of 13 nm was produced, and was stored at 4ºC.

Diameter of the prepared 13 nm AuNPs was measured by a scanning electron microscope (SEM) and dynamic light scattering (DLS) particle size analyzer. Moreover, the absorption spectrum of AuNPs was measured by a spectrophotometer (SpectraMax 190; Molecular Devices Corporation, Sunnydale, CA, USA).

3-2-2 Modification of AuNPs/MCH-gelatin

The process of modified gelatin and MCH on AuNPs were monitored by observing the spectral change after the addition of gelatin and MCH to colloidal AuNPs. The gelatin and MCH were attached to the AuNPs according to below procedures:

The 50 μL of aqueous gelatin solution (0.1%) was added to 950 μL of the aqueous 13 nm AuNPs solution. After careful mixing, the mixture was incubated and shaken at 37°C for 2 hr. The mixture was then centrifuged for 6 min at 14,000 × *g* to remove the excess gelatin. After two centrifuge/wash cycles, the colloids was resuspended in 200 μL of NTTC buffer (50 mM NaCl, 50 mM Tris-HCl, 5 mM $CaCl_2$, and 0.05 % Triton X-100, pH 7.5), and this colloid solution was regarded as AuNPs/gelatin. The synthesis procedure of AuNPs/MCH-gelatin was similar with AuNPs/gelatin. After 950 μL AuNPs solution and gelatin (0.1%, 50 μL) incubated at 37°C for 2 hr, 10 μL of MCH (1 mM) was added into the solution. After

vortexing, the mixture was incubated and shaken at 37°C for another 2 hr. The mixture was then centrifuged for 6 min at 14,000 × *g* to remove the excess gelatin and MCH. After two centrifuge/wash cycles, the colloid solution was resuspended in 200 μL of NTTC buffer, and this colloid was regarded as AuNPs/MCH-gelatin.

3-3 Confirm size and morphology change of AuNPs/MCH-gelatin

3-3-1 Dynamic light scattering

Dynamic light scattering (DLS; also known as Photon Correlation Spectroscopy or Quasi-Elastic Light Scattering) is a technique which can be used to determine the size distribution of small particles in solution. The method utilizes laser as light source which is monochromatic and coherent, and observes a time-dependent fluctuation in the scattering light intensity to determine the translational diffusion coefficient of small particles.

The AuNPs samples were diluted with NTTC buffer (filtered through 0.45 μm syringe filters) and filled into the light scattering cuvette. Light scattering experiments were performed using the BI-200SM Goniometer (Brookhaven Instruments Corporation, Holtsville, NY, USA) at a temperature of 20°C. The laser wavelength was 532 nm, and measurements were conducted at an angle of 90°. The DLS data were analyzed by Brookhaven Instruments-Dynamic Light Scattering software.

3-3-2 Scanning electron micrographs

High resolution scanning electron microscopic (SEM) images of modified-AuNPs were obtained with a field-emission SEM instrument JSM-6700F (JEOL, Tokyo, Japan) and operated at 15 kV. The samples were prepared by dropping 10 μl of AuNPs solution onto a

gold chip and incubated samples at 37°C for 30 min. Finally, the chips were rinsed thoroughly with distilled water and air-dried for scanning.

3-3-3 The electrophoresis analysis of modified-AuNPs

To observe the size change of modified-AuNPs which digested by proteinase, the gel electrophoresis was used to separate AuNPs according to the gelatin of attached.

Agarose gel 0.5 % (w/v) was prepared with and immersed in 0.5 X TBE buffer (Tris-Borate-EDTA buffer, prepared by diluting 10 x stock solutions). The gel was run in a horizontal electrophoresis system (Mini-Sub Cell GT, Biorad, electrode spacing 15 cm). The gel image was recorded by a consumer digital camera and processed the images only with small linear contrast adjustments in order to give a true representation of the visual gel appearance.

Before loading the gel of the modified-AuNPs samples, the modified-AuNPs were coated with a layer of sodium dodecyl sulfate (SDS) which imparts a negative charge on the gelatin of AuNPs, and forced all of modified-AuNPs run to positive electrode. After trypsin digested at 37°C for 10 min, each of digested-AuNPs samples was loaded into one well of the gel, and the gel was ran for 30 min at 110 V in 0.5 X TBE buffer.

3-4 Investigation the stability of AuNPs/MCH-gelatin

To study the stability of AuNPs/MCH-gelatin in strict envionmrnt, 50 μL of different buffer solution was added into 200 μL of AuNPs/MCH-gelatin solution. The 1N HCl and the 1N NaOH were used to analyze the stability of AuNPs/MCH-gelatin under extreme pH

condition, and 10 X PBS buffer (1,370 mM NaCl, 27 mM KCl, 100 mM Na_2HPO_4, 20 mM KH_2PO_4, pH 7.4) was used to analyze the influence of high salt concentration buffer on AuNPs/MCH-gelatin. As a control, 50 μl of NTTC buffer solution was mixed with 200 μL of AuNPs/MCH-gelatin. All of samples were incubated at 37°C for 30 min, and the absorbance wavelength was analyzed with UV-Vis absorption spectrophotometer.

3-5 Assay of proteinase activity

3-5-1 Activation of MMP-2

Preliminary experiments were undertaken to determine the concentrations MMP-2 required for maximal activation of each sample. The lyophilized powder MMP-2 was resuspended in 0.1 mL of TCNB buffer (composed of 50 mM Tris, 10 mM $CaCl_2$, 150 mM $NaCl_2$, and 0.05% triton-X100, pH 7.5), and activated by *p*-Aminophenylmercuric acetate (APMA).

APMA is an organomercurial agent used for the activation of latent MMPs *in vitro*. The procedure for activation was as follows: The stock solution of APMA was prepared by dissolve 3.5 mg APMA in 1 mL 0.1 M NaOH, this stock solution should be 10 mM. Then neutralize the high base by diluting 4 folds in Tris-Triton-Calcium buffer (50 mM Tris-HCl, 1 mM CaCl2, 0.05% triton X-100 pH 7.5). For activated MMP-2, the APMA solution was mix with MMP-2 sample to give a final concentration of 0.25 mM. Then activation times will vary depending upon the samples. MMP-2 generally requires short activation time. In this study, MMP-2 samples were activated at 37°C for 2 hr. This final activated MMP-2 solution can be used directly without dialyzing away the APMA [Sellers et al., 1977].

3-5-2 Proteinase activity assay by AuNPs-based optical biosensing platform

For the assay of proteinase activity, the measurement were performed in NTTC buffer as a control experiment and observed result. NTTC buffer would not influence the absorbance of AuNPs, and NTTC buffer would not promote the AuNPs/MCH-gelatin to aggregate. The concentration of gelatin modified-AuNPs was adjusted to 5 nM for the further assay of proteinase activity. In the proteinase activity assay, an amount of 50 μL trypsin or MMP-2 samples solution with different concentrations was added into 200 μL of modified-AuNPs and then the mixture was incubated at 37°C. The activity of MMP-2 were much lower than the ones of trypsin, in order to amplify the detection signal of MMP-2, the incubation time was adjusted to 30 min. After proteinase digested, 200 μL of mixture solutions were transferred into 96-well plate. All of samples were analyzed with UV-Vis absorption spectrophotometer and recorded their wavelength and $A_{625\ nm}/A_{525\ nm}$. The tests were performed in triplates.

3-5-3 Proteinase activity assay by zymography

The activated MMP-2 solution was mixed with zymography buffer (composed of 0.5 M Tris-HCl, pH 6.8, glycerol, 10% (w/v) SDS, and 0.1% bromophenol blue) and stood at room temperature for 10 min. Then loaded on 8% SDS-polyacrylamide gel containing 0.1 mg/mL gelatin, and ran the gel with Tris-Glycine SDS running buffer at 80 V for 4 hr.

Following electrophoresis, the gel was washed twice in renaturing buffer (2.5% trixton X-100) with gentle agitation at room temperature for 30 min in order to exchange SDS to Triton-X100. And decant the renaturing buffer, then replaced with developing buffer (50 mM Tris-HCl, pH 7.4, 200 mM NaCl, and 5 mM $CaCl_2$) at room temperature for 30 min, then replaced with fresh developing buffer and incubated at 37°C for 18 hr.

The gel was stained with coomassie staining solution (0.125% Coomassie Brilliant Blue

R250, 50% (v/v) methanol, 10% (v/v) acetic acid) for 30 min, then was destained with destain buffer (25% (v/v) methanol, 7.5% (v/v) acetic acid in ddH_2O).

Gelatinolytic activities were identified as clear bands against a dark blue background where the protease has digested the substrate. Gelatinase activities in the gels were quantified using Scion imageTM which quantifies both the surface and the intensity of lysis bands after scanning the gel [Stawowy et al., 2004].

3-6 Assay the efficiency of MMPs inhibitors

In order to apply for drug screening, two broad-spectrum MMP inhibitors were used in this study. MMPIs are synthetic molecules and behave as MMPs competitive inhibitors [Augé et al., 2004]. Galardin is a potent hydroxamate-type MMP inhibitor with a broad inhibitory profile. ONO-4817 is a novel synthetic hydroxamic acid-based nonpeptide compound designed to be administered orally. ONO-4817 binds reversibly to the zinc-binding region of MMPs and has a selective inhibitory spectrum [Yamamoto et al., 2003]. Both of them have been used to inhibit the MMP-2 activity through binding to its active site and develope the treatment of MMP-related diseases [Galardy et al., 1994; Yamada et al., 2000; Yamamoto et al., 2003; Bai et al., 2005].

3-6-1 Assay the efficiency of MMPs inhibitors by AuNPs-based optical biosensing platform

For drug screening assay of MMP-2, the procedure was similar with proteinase activity assay. In this inhibitors screening assay, 50 μL of MMP-2 (250 ng/mL) with different concentrations of inhibitor was added into 200 μL of AuNPs/MCH-gelatin (5nM) and the

mixtures were incubated at 37°C for 30 min. Finally, the mixture solution was transferred into 96-well plate, then the color change and UV-Vis absorption spectra were collected by SpectraMax 190 UV-Vis spectrophotometer. $A_{625\ nm}/A_{525\ nm}$ of AuNPs/MCH-gelatin was used to quantitatively estimate the inhibitors activity.

3-6-2 Assay the efficiency of MMPs inhibitors by zymograph

The condition of zymography electrophoresis for inhibitors screening was the same as previously narrated except the composition of developing buffer. After washed twice in renaturing buffer and replaced with developing buffer for 30 min, the gel was replaced with fresh developing buffer which was added with different concentrations of inhibitor and incubated at 37°C for 48 hr. Finally, the gel was stained with coomassie staining solution, and then was destained with the destain buffer.

IV. Results and Discussion

4-1 Synthesis of AuNPs and AuNPs/MCH-gelatin

In the study, the 13 nm AuNPs was used to establishing an optical biosensing platform to assay proteinase activity. The 13 nm AuNP was produced by sodium citrate reduction method. The absorption spectra of 13 nm AuNPs and modified-AuNPs (AuNPs/gelatin and AuNPs/MCH-gelatin) were scanned by Ultrospec 3300 pro UV-Vis spectrophotometer (Amersham Biosciences). The extinction coefficients of the AuNPs are normally very high [Jena and Raj, 2008]. In the previous reports, the optical spectrum was used to estimate the particles size of AuNPs, and the maximum absorbance (λ_{max}) of 13 nm AuNPs was located at 520nm [Elghanian et al., 1997].

Figure 4-1 shows the UV-Vis absorption spectra of 13 nm AuNPs, AuNPs/gelatin and AuNPs/MCH-gelatin. The red-colored AuNPs (13nm in diameter) had surface plasmon resonance band at 520 nm. When the 13 nm AuNPs was modified with gelatin, the particles size was increased, and the λ_{max} of AuNPs/gelatin shifted from 520 to 525 nm. In addition, the absorption peak at 280 nm was correspondent to the absorption from functional group of amino acid. The UV-Vis spectrum of AuNPs/MCH-gelatin was similar to AuNPs/gelatin, and both of their λ_{max} was located at 525 nm. Owing to the MCH as a small compound, when AuNPs was modified with MCH, the particles size of AuNPs had no significant change, and the λ_{max} of AuNPs/MCH-gelatin did not shift. Nevertheless, compared AuNPs/MCH-gelatin with AuNPs/gelatin, the surface plasmon (SP) band of AuNPs/MCH-gelatin was broader than AuNPs/gelatin. Jena and Raj reported that the SP band depends on the shape, size and the surrounding medium of the particle [Jena and Raj, 2008]. The results revealed that the size of AuNPs/MCH-gelatin was similar with AuNPs/gelatin, but the physical property of AuNPs/MCH-gelatin was different from

AuNPs/gelatin.

From the data, after appropriate curve fitting and subtraction of the spectrum from the AuNPs absorption, the concentrations of AuNPs could be calculate from the absorbance by used the Beer–Lambert law:

$$\text{Absorbance} = \varepsilon bc$$

where ε is molar extinction coefficient, b is the path length of the sample, and c is molar concentration. The ε of 13 nm AuNPs at λ_{520} is 2.7×10^8/M cm [Jin et al., 2003]. By using the Beer–Lambert law, the concentration of modified-AuNPs were calculated, and modified-AuNPs was adjusted to 5 nM for the further assay of proteinase activity.

4-2 Identification of the size and morphology change of modified-AuNPs

The size change of modified-AuNPs was investigated by DLS (**Figure 4-2**) and the morphology change of modified-AuNPs was observed by SEM (**Figure 4-3**). In the process of the 13 nm AuNPs synthesized by sodium citrate reduction, citrate ions and free chloride ions were adsorbed on the surface to AuNPs, and provided negative charge to AuNPs surface [Saraiva and de Oliveira, 2002]. The non-modified AuNPs was dispersive on the chip (**Figure 4-3**) due to the negative charge of AuNPs would repel each other, and the average particles size of non-modified AuNPs was about 13.3 nm (**Figure 4-2 A**).

When the 13 nm AuNPs was modified with gelatin (whether MCH was modified on AuNPs later or not), the gelatin increased the steric repulsion of AuNPs which can prevented the AuNPs from aggregation (**Figure 4-3**), and the diameter of AuNPs/gelatin and

AuNPs/MCH-gelatin was estimated about 35.5 nm and 37.2 nm, respectively (**Figure 4-2**).

After proteinase digested the AuNPs/gelatin, AuNPs/gelatin showed slightly aggregated (**Figure 4-3 C**) due to the steric repulsion generated by gelatin was too difficult to overcome. In contrast, as shown in **Figure 4-3 E**, while AuNPs/MCH-gelatin was digested by proteinase, MCH increased the attraction among the AuNPs and resulted in a dramatic aggregation. Moreover, the DLS data shown in **Figure 4-2** was similar with the results in SEM assay. Nevertheless, the size of AuNPs samples measured by DLS would larger than that obtained from SEM study, which was mainly because DLS measures the hydrodynamic radius while SEM provided a more precise measurement of the hard AuNPs core.

4-3 The electrophoresis mobility of modified-AuNPs

The technique of gel electrophoresis was successfully used to separate modified-AuNPs according to particles size. The modified-AuNPs were digested by trypsin for 10 min, and ran the sample in 0.5% agarose gel for 30 min. The electrophoresis mobility of modified-AuNPs was showed in **Figure 4-4.** In **Figure 4-4**, the non-modified AuNPs was move fastest in the agarose gel due to the particles size of bare AuNPs was smallest compared with other modified-AuNPs.

After trypsin digested, the particles size of modified-AuNPs decreased, and the electrophoresis mobility of those digested-AuNPs increased. However, the particles size of digested-AuNPs was still larger than bare ones, which indicated that the trypsin did not cleavage the gelatin on the surface of AuNPs completely. In contrast to AuNPs/gelatin, after trypsin digested, the AuNPs/MCH-gelatin aggregated and was difficult to move in agarose gel. For this result, some aggregated-AuNPs remain stayed upon gel and resulted in one black

band. Consequently, a few no aggregation AuNPs/MCH-gelatin could move toward anode. Therefore, the mobility of AuNPs in the gel was strongly depending on the particles size of AuNPs.

4-4 Effects of MCH on AuNPs-based optical biosensing platform

The **Figure 4-5** was revealed the effect of MCH on AuNPs-based optical biosensing platform. After trypsin was added into AuNPs/gelatin, the λ_{max} at 525 nm was slightly decreased, the spectrum of AuNPs/gelatin without significant red shift, and no defectable color change (**Figure 4-5A**). However, while trypsin was added into AuNPs/MCH-gelatin, the λ_{max} around 525 nm decreased conspicuously and emerged an absorbance band among 600 nm to 650 nm. The color of the solution changed from wine-red to violet-purple, and could be visuzlized by naked eye (**Figure 4-5B**).

The difference between AuNPs/gelatin and AuNPs/MCH-gelatin was the function groups of MCH could enhance the attraction between AuNPs and overcome the steric stabilization induced by gelatin, resulted in the aggregation and the color of AuNPs/MCH-gelatin changed from wine-red to violet-purple.

Time-dependent changed of absorbance spectrum of AuNPs-based optical biosensing platform was shown in **Figure 4-6**. After trypsin digested the substrate of AuNPs/MCH-gelatin, the absorption band around 525 nm decreased gradually, and concomitantly, a new broad absorption above 625 nm emerged and its intensity increased by prolonging the reaction time. The new broad absorption above 625 nm emerged was due to the AuNPs/MCH-gelatin began aggregation and resulted in a red shift of absorption spectrum.

Figure 4-7 showed the optimum MCH concentration on AuNPs-based optical biosensing

platform. Increasing amounts of MCH caused increased red shifting of the absorbance spectrum of AuNPs/MCH-gelatin, due to the MCH could enhance the attraction between AuNPs and cause the AuNPs/MCH-gelatin to aggregate. MCH played an important role as an inducer when the MCH concentration above 6 μM (**Figure 4-7B)**. As the concentration of MCH increased, the response time for AuNPs/MCH-gelatin to aggregate decreased, and the concentration above 15 μM was caused a hasty aggregation. Therefore, the 10 μM MCH was used to modify on the surface of AuNPs as inducer and blocker to establish an AuNPs-based optical biosensing platform for assay proteinase activity, and the absorption ratio ($A_{625\ nm}/A_{525\ nm}$) of AuNPs/MCH-gelatin was used to quantity estimate the proteinase activity.

4-5 The stability of AuNPs/MCH-gelatin

When enzymes carry out their function, changing in the niche (such as pH, temperature, metal ion or salt concentration) would affect the activity of enzymes. In addition, AuNPs would begain aggregate when the pH or the buffer salt concentration changed. To explore the stability of AuNPs/MCH-gelatin, the AuNPs/MCH-gelatin was applied into different buffer solutions. When AuNPs modified with gelatin and MCH, the gelatin increased the steric repulsion of AuNPs, and prevented the AuNPs surfaces coming into close contact. For this reason, the AuNPs/MCH-gelatin exhibited a dramatic stability in strict environment (pH 1, pH 13 or high salt concentration). The λ_{max} and waveform of AuNPs/MCH-gelatin were no change in different buffer condition (**Figure 4-8**). Consequently, the system could detect enzyme activity in niche environment which for maximum activity of the enzyme.

4-6 Assay of proteinase activity

4-6-1 Assay of trypsin activity by AuNPs-based optical biosensing platform

Trypsin is a serine proteinase found in the digestive system of many vertebrates; it predominantly cleaved peptide chains at the carboxyl side of the amino acids lysine and arginine, except when either is followed by proline. Trypsin has been applied in many biotechnological processes, such as used in cell culture to resuspend cells or in biological research during proteomics experiments to digest proteins.

In this study, the AuNPs/MCH-gelatin was used to assay the trypsin activity. The 5 nM of AuNPs/MCH-gelatin solutions were incubated with different concentrations of trypsin (from 5×10^{-2} U to 5×10^{3} U) at 37°C for 10 min. As the concentrations of trypsin raising, the aggregation degree of AuNPs/MCH-gelatin increased, and resuted in a remarkable color change from wine-red to purple (**Figure 4-9**). In addition, large absorption spectra variation would be observed (**Figure 4-10 A**). To estimate the activity of trypsin, the ratios of the absorbance at 625 and 525 nm ($A_{625\ nm}/A_{525\ nm}$) at 10 min after the addition of trypsin were plotted as a function of trypsin concentration (**Figure 4-10 B**). These two absorbances were chosen to represent the relative amount of aggregating and suspending AuNPs, respectively.

When plotting $A_{625\ nm}/A_{525\ nm}$ against the trypsin concentration, it is found that the correlation coefficients (R^2) was 0.9733 for the determination of trypsin in the concentration ranges from 5×10^{-1} U to 5×10^{2} U, and the detection limit of this method could reach to as low as 5×10^{-1} U for trypsin.

4-6-2 Assay of MMP-2 activity by AuNPs-based optical biosensing platform

This AuNPs-based optical biosensing platform also can assay MMP-2 activity, and the

procedure was the same as trypsin activity assay. When extend the detection time from 10 min to 30 min, the detection limit of this system can reach 50 ng/mL for MMP-2, and has a linear relation between 50 to 600 ng/mL (y = 0.0009x + 0.2341, R^2 = 0.9874) (**Figure 4-11**).

4-6-3 Assay of MMP-2 activity by zymography

Gelatin zymography was also used to detection of the MMP-2 activity (**Figure 4-12**), and has a linear relationship between 10 ng/mL to 700 ng/mL (y = 0.0497x + 1.2533, R^2 = 0.9912).

4-7 Assay the efficiency of MMPs inhibitors

This convenient AuNPs-based optical biosensing platform was further applied for MMP-2 inhibitor screening. Galardin and ONO-4817, two well-known inhibitors for MMP-2 were selected as examples to demonstrate the application in MMP-2 inhibitor screening. The AuNPs/MCH-gelatin solutions containing MMP-2 (250 ng/mL) and presence of different concentrations of MMP-2 inhibitors were measured after the solutions were incubated at 37 for 1 hr.

In the presence of an efficient inhibitor in the AuNPs/MCH-gelatin solution, no detectable color change occurs, and the solutions are indefinitely stable without showing signs of aggregation. These results can be accountable, since galardin and ONO-4817 can inhibit the activity of MMP-2, the aggreation of AuNPs/MCH-gelatin will become slow, and resulted in less absorption variation (and less color change). **Figure 4-13** displays the $A_{625\ nm}/A_{525\ nm}$ which obtained during the MMPs inhibitors to block the MMP-2 activity. The half maximal inhibitory concentration (IC_{50}; Concentration of inhibitor that reduces enzyme activity to 50%

of the activity of the native enzyme) were estimated by calculate the $A_{625\ nm}/A_{525\ nm}$ of AuNPs/MCH-gelatin. Comparison ONO-4817 with galardin, galartin had better efficiency than ONO-4817. The galardin and ONO-4817 inhibition with MMPs activity for IC_{50} values were 1.87 nM and 17.76 nM, respectively.

The efficiency of MMP-2 inhibitors was also analyzed by zymography (**Figure 4-14**) and the IC_{50} values were estimated to be 3.48 and 14.33 nM for galardin and ONO-4817, respectively. The data of AuNPs-based optical biosensing platform was consistent with zymography. Nevertheless, comparing this platform with zymograpgy, high surface-to-volume area of AuNPs provided more space that can not only enhance the immobilization density of gelatin, but also raised the chance for MMP-2 to digest gelatin. The detection time for zymography to screening the inhibitor of MMP-2 needs 24 hr at least; however, the platform can shorten detection time to 1 hr. On the other hand, when zymography was used to analyze the activity of MMP-2, the SDS would active MMP-2 and original activity of MMP-2 would change, but the activity of MMP-2 would not be changed when AuNPs-based optical biosensing platform was used. Therefore, the AuNPs-based optical biosensing platform not only possible to perform a colorimetric assay for proteinase activity, but also has potential for further applications in anti-MMPs drugs screening.

V. Conclusions

In this study, the AuNPs/MCH-gelatin was synthesized by combining 13 nm AuNPs, gelatin and MCH. Moreover, the AuNPs/MCH-gelatin was used to establish a simple and specific AuNPs-based optical biosensing platform for real-time and rapid assay of proteinase activity and inhibitor screening.

The key technology for this platform was using MCH as inducer and blocker. In previous reports, MCH was only used as blocker to prevent non-specific binding, but we first found that MCH was also an effective compound which can reinforce the attraction force between AuNPs. In this study, when AuNPs/MCH-gelatin surface substrate digested by proteinase, AuNPs/MCH-gelatin lost the steric stability and the interparticle distance shortened, followed by a rapid gathering phenomenon. The aggregation of AuNPs would change their optical property, i.e. plasmon resonance, and could be detected by visualizing in solution as color changes from red to purple with naked eye or using UV-Vis spectroscopy to quantify accurately the concentration of proteinase.

Using the low-cost platform of AuNPs, the linear range of trypsin detection by the AuNPs-based optical biosensing platform was from 5×10^{-1} to 5×10^{2} U and with a detection limit of 5×10^{-1} U. A linear correlation was established when the MMP-2 activity was from 50 ng/mL to 600 ng/mL, and with a detection limit of 50 ng/mL. Furthermore, the result of this AuNPs-based method for MMP-2 inhibitor drugs screening study was in agreement with zymography method.

The simple screening method not only offers an alternative platform to assay of proteinase activity, also can be application in high-throughput screening of MMPs inhibitors and relevant drug discovery.

VI. References

Albrecht-Buehler G. 1979. The angular distribution of directional changes of guided 3T3 cells. *The Journal of Cell Biology* 80:53-60.

Alocilja E, Muhammad-Tahir Z. 2008. Label-free microbial biosensors using molecular nanowire transducers. *Principles of Bacterial Detection: Biosensors, Recognition Receptors and Microsystems* 377-413.

Allgayer H, Babic R, Beyer BC, Grützner KU, Tarabichi A, Schildberg FW, Heiss MM. 1998. Prognostic relevance of MMP-2 (72-kD collagenase IV) in gastric cancer. *Oncology* 55:152-160.

Augé F, Hornebeck W, Laronze JY. 2004. A novel strategy for designing specific gelatinase A inhibitors: potential use to control tumor progression. *Critical Reviews in Oncology Hematology* 49:277-282.

Bai S, Thummel R, Godwin AR, Nagase H, Itoh Y, Li L, Evans R, McDermott J, Seiki M, Sarras MP Jr. 2005. Matrix metalloproteinase expression and function during fin regeneration in zebrafish: Analysis of MT1-MMP, MMP2 and TIMP2. *Matrix Biology* 24:247-260.

Bando E, Yonemura Y, Endou Y, Sasaki T, Taniguchi K, Fujita H, Fushida S, Fujimura T, Nishimura G, Miwa K, Seiki M. 1998. Immunohistochemical study of MT-MMP tissue status in gastric carcinoma and correlation with survival analyzed by univariate and multivariate analysis. *Oncology Reports* 5:1483-1488.

Bergers G, Brekken R, McMahon G, Vu TH, Itoh T, Tamaki K, Tanzawa K, Thorpe P, Itohara S, Werb Z, Hanahan D. 2000. Matrix metalloproteinase-9 triggers the angiogenic switch during carcinogenesis. *Nature Cell Biology* 2:737-744.

Bergveld P. 1996. The future of biosensors. *Sensors and Actuator A: Physical* 56:65-73.

Birkedal-Hansen H, Moore WG, Bodden MK, Windsor LJ, Birkedal-Hansen B, DeCarlo A, Engler JA. 1993. Matrix metalloproteinases: a review. *Critical Reviews in Oral Biology and Medicine* 4:197-250.

Birkedal-Hansen H, Taylor RE. 1982. Detergent-activation of latent collagenase and resolution of its component molecules. *Biochemical and Biophysical Research Communications* 107:1173-1178.

Bollmann M, Bankfalvi A, Trosic A Speich N, Schmittt C, Bollmann R. 2005. Can we detect cervical human papillomavirus (HPV) infection by cytomorphology alone? Diagnostic value of non-classic cytological signs of HPV effect in minimally abnormal Pap tests. *Cytopathology* 16:13-21.

Boozer C, Ladd J, Chen S, Yu Q, Homola J, Jiang S. 2004. DNA directed protein immobilization on mixed ssDNA/oligo(ethylene glycol) self-assembled monolayers for sensitive biosensors. *Analytical Chemistry* 76:6967-6972.

Brew K, Dinakarpandian D, Nagase H. 2000. Tissue inhibitors of metalloproteinases: evolution, structure and function. *Biochimica et Biophysica Acta* 1477:267-283.

Brust M, Walker M, Bethell D, Schiffrin DJ, Whyman R. 1994. Synthesis of thiol-derivatised gold nanoparticles in a two-phase Liquid–Liquid system. *Journal of the Chemical Society, Chemical Communications* 801-802.

Buchmueller KL, Staples AM, Uthe PB, Howard CM, Pacheco KA, Cox KK, Henry JA, Bailey SL, Horick SM, Nguyen B, Wilson WD, Lee M. 2005. Molecular recognition of DNA base pairs by the formamido/pyrrole and formamido/imidazole pairings in stacked polyamides. *Nucleic Acids Research* 33:912-921.

Bui MP, Baek TJ, Seong GH. 2007. Gold nanoparticle aggregation-based highly sensitive DNA detection using atomic force microscopy. *Analytical and Bioanalytical Chemistry* 388:1185-1190.

Campbell B, Lei J, Kiaei D, Sustarsic D, Shami S. 2004. Nucleic acid testing using surface plasmon resonance fluorescence detection. *Clinical Chemistry* 50:1942-1943.

Cao YC, Jin R, Thaxton CS, Mirkin CA. 2005. A two-color-change, nanoparticle-based method for DNA detection. *Talanta* 67:449-455.

Carmeli E, Moas M, Reznick AZ, Coleman R. 2004. Matrix metalloproteinases and skeletal muscle: a brief review. *Muscle and Nerve* 29:191-197.

Caruso RA, Ashokkumar M, Griese F. 2002. Sonochemical formation of gold sols. *Langmuir* 18:7831-7836.

Castañeda MT, Merkoçi A, Pumera M, Alegret S. 2007. Electrochemical genosensors for biomedical applications based on gold nanoparticles. *Biosensors and Bioelectronics* 22:1961-1967.

Cavalcanti A, Shirinzadeh B, Zhang M, Kretly LC. 2008. Nanorobot hardware architecture for medical defense. *Sensors* 8:2932-2958.

Che Y, Li Y, Slavik M. 2001. Detection of Campylobacter jejuni in poultry samples using an enzyme-linked immunoassay coupled with an enzyme electrode. *Biosensors and Bioelectronics* 16:791-797.

Chenard MP, O'Siorain L, Shering S, Rouyer N, Lutz Y, Wolf C, Basset P, Bellocq JP, Duffy MJ. 1996. High levels of stromelysin-3 correlate with poor prognosis in patients with breast carcinoma. *International Journal of Cancer* 69:448-451.

Chen SH, Wu VC, Chuang YC, Lin CS. 2008. Using oligonucleotide-functionalized Au nanoparticles to rapidly detect foodborne pathogens on a piezoelectric biosensor. *Journal of Microbiological Methods* 73:7-17.

Chen SJ, Huang YF, Huang CC, Lee KH, Lin ZH, Chang HT. 2008. Colorimetric determination of urinary adenosine using aptamer-modified gold nanoparticles. *Biosensors and Bioelectronics* 23:1749-1753.

Chen YM, Yu CJ, Cheng TL, Tseng WL. 2008. Colorimetric detection of lysozyme based on electrostatic interaction with human serum albumin-modified gold nanoparticles. *Langmuir* 24:3654-3660.

Chen YT, Hsu CL, Hou SY. 2008. Detection of single-nucleotide polymorphisms using gold nanoparticles and single-strand-specific nucleases. *Analytical Biochemistry* 375:299-305.

Cheng TJ, Sung MT, Liao HY, Chang YF, Chen CW, Huang CY, Chou LY, Wu YD, Chen YH, Cheng YS, Wong CH, Ma C, Cheng WC. 2008. Domain requirement of moenomycin binding to bifunctional transglycosylases and development of high-throughput discovery of antibiotics. *Proceedings of the National Academy of Sciences of the United States of America* 105:431-436.

Cho YK, Kim S, Kim YA, Lim HK, Lee K, Yoon D, Lim G, Pak YE, Ha TH, Kim K. 2004. Characterization of DNA immobilization and subsequent hybridization using in situ quartz crystal microbalance, fluorescence spectroscopy, and surface plasmon resonance. *Journal of Colloid and Interface Science.* 278:44-52.

Chithrani BD, Chan WC. 2007. Elucidating the nechanism of cellular uptake and removal of protein-coated gold nanoparticles of fifferent sizes and shapes. *Nano Letters* 7:1542-1550.

Chithrani BD, Ghazani AA, Chan WC. 2006. Determining the size and shape dependence of gold nanoparticle uptake into mammalian cells. *NanoLetters* 6:662-668.

Clark LCJr, Lyons C. 1962. Electrode systems for continuous monitoring in cardiovascular surgery. *Annals of the New York Academy of Sciences* 102:29-45.

Coker ML, Doscher MA, Thomas CV, Galis ZS, Spinale FG. 1999. Matrix metalloproteinase synthesis and expression in isolated LV myocyte preparations. *The American Journal of Physiology* 277:H777-H787.

Compagnone D, Esti M, Messia MC, Peluso E, Palleschi G. 1998. Development of a biosensor for monitoring of glycerol during alcoholic fermentation. *Biosensors and Bioelectronics* 13:875-880.

Cosnier S, Gondran C, Dueymes C, Simon P, Fontecave M, Décout JL. 2004. New flavin and deazaflavin oligonucleotide conjugates for the amperometric detection of DNA hybridization. *Chemical Communications (Cambridge, England)* 21:1624-1625.

Cox G, Jones JL, O'Byrne KJ. 2000. Matrix metalloproteinase 9 and the epidermal growth factor signal pathway in operable non-small cell lung cancer. *Clinical Cancer Research* 6:2349-2355.

Craig VSJ , Ninham BW, Pashley RM. 1998. Comment on ‘‘Deformation of fluid interfaces under double-layer forces stabilizes bubble dispersions’’. *Physical Review E* 57:7362-7363.

Davidson B, Goldberg I, Kopolovic J, Lerner-Geva L, Gotlieb WH, Ben-Baruch G, Reich R. 1999. MMP-2 and TIMP-2 expression correlates with poor prognosis in cervical carcinoma-a clinicopathologic study using immunohistochemistry and mRNA in situ hybridization. *Gynecologic Oncology* 73:372-382.

Davidson B, Goldberg I, Gotlieb WH, Kopolovic J, Ben-Baruch G, Nesland JM, Berner A, Bryne M, Reich R. 1999. High levels of MMP-2, MMP-9, MT1-MMP and TIMP-2 mRNA correlate with poor survival in ovarian cancer. *Clinical and Experimental Metastasis* 17:799-808.

Davidson W, Frego L, Peet GW, Kroe RR, Labadia ME, Lukas SM, Snow RJ, Jakes S, Grygon CA, Pargellis C, Werneburg BG. 2004. Discovery and characterization of a substrate selective p38alpha inhibitor. *Biochemistry* 43:11658-11671.

Davis F, Nabok AV, Higson SP. 2005. Species differentiation by DNA-modified carbon

electrodes using an ac impedimetric approach. *Biosensors and Bioelectronics* 20:1531-1538.

de la Fuente JM, Berry CC. 2005. Tat peptide as an efficient molecule to translocate gold nanoparticles into the cell nucleus. *Bioconjugate Chemistry* 16:1176-1180.

De M, Ghosh PS, Rotello VM. 2008. Applications of nanoparticles in biology. *Advanced Materials* 20:4225-4241.

De Mey J, Lambert AM, Bajer AS, Moeremans M, De Brabander M. 1982. Visualization of microtubules in interphase and mitotic plant cells of aemanthus endosperm with the immuno-gold staining method. *Proceedings of the National Academy of Sciences of the United States of Americ*a 79:1898-1902.

Dickinson TA, White J, Kauer JS, Walt DR. 1996. A chemicaldetecting system based on a cross-reactive optical sensor array. *Nature* 382:697-700.

Du D, Ding J, Cai J, Zhang A. 2007. Determination of carbaryl pesticide using amperometric acetylcholinesterase sensor formed by electrochemically deposited chitosan. *Colloids and Surfaces B, Biointerfaces* 58:145-150.

Dulkeith E, Morteani AC, Niedereichholz T, Klar TA, Feldmann J, Levi SA, van Veggel FC, Reinhoudt DN, Möller M, Gittins DI. 2002. Fluorescence quenching of dye molecules near gold nanoparticles: radiative and nonradiative effects. *Physical Review Letters* 89:203002.

Dutra RF, Mendes RK, Lins da Silva V, Kubota LT. 2007. Surface plasmon resonance immunosensor for human cardiac troponin T based on self-assembled monolayer. *Journal of Pharmaceutical and Biomedical Analysis* 43:1744-1750.

Elghanian R, Storhoff JJ, Mucic RC, Letsinger RL, Mirkin CA. 1997. Selective colorimetric detection of polynucleotides based on the distance-dependent optical properties of gold nanoparticles. *Science* 277:1078-1081.

Etoh T, Inoue H, Yoshikawa Y, Barnard GF, Kitano S, Mori M. 2000. Increased expression of collagenase-3 (MMP-13) and MT1-MMP in eosophageal cancer is related to cancer aggressiveness. *Gut* 47:50-56.

Faulk WP, Taylor GM. 1971. Communication to the editors: An immunocolloid method for the electron microscope. *Immunochemistry* 8:1081-1083.

Fedarko NS, Jain A, Karadag A, Fisher LW. 2004. Three small integrin binding ligand N-linked glycoproteins (SIBLINGs) bind and activate specific matrix metalloproteinases. *The FASEB Journal* 18:734-736.

Feriotto G, Breveglieri G, Gardenghi S, Carandina G, Gambari R. 2004. Surface plasmon resonance and biosensor technology for real-time molecular diagnosis of beta o 39 thalassemia mutation. *Molecular Diagnosis* 8:33-41.

Ferreira LS, De Souza MBJr, Trierweiler JO, Broxtermann O, Folly ROM, Hitzmann B. 2003. Aspects concerning the use of biosensors for process control: experimental and simulation investigations. *Computers and Chemical Engineering* 27:1165-1173.

Fojta M, Havran L, Kizek R, Billova S, Palecek E. 2004. Multiply osmium-labeled reporter probes for electrochemical DNA hybridization assays: detection of trinucleotide repeats.

Biosensors and Bioelectronics 20:985-994.

Foulds NC and Lowe CR .1985. Whats new: biosensors: current applications and future potential. *BioEssays* 3:129-132.

Frens G. 1973. Controlled nucleation for the regulation of the particle size in monodisperse gold suspensions. *Nature Physics* 241:20-22.

Fu Y, Yuan R, Xu L, Chai Y, Liu Y, Tang D, Zhang Y. 2005. Electrochemical impedance behavior of DNA biosensor based on colloidal Ag and bilayer two-dimensional sol-gel as matrices. *J Biochem Biophys Methods* 62:163-174.

Galardy RE, Grobelny D, Foellmer HG, Fernandez LA. 1994. Inhibition of angiogenesis by the matrix metalloprotease inhibitor N-[2R-2-(hydroxamidocarbonymethyl)-4-methylpentanoyl)]-L-tryptophan methylamide. *Cancer Research* 54:4715-4718.

Galazka G, Windsor LJ, Birkedal-Hansen H, Engler JA. 1996. APMA (4-aminophenylmercuric acetate) activation of stromelysin-1 involves protein interactions in addition to those with cysteine-75 in the propeptide. *Biochemistry* 35:11221-11227.

Geng T, Morgan MT, Bhunia AK. 2004. Detection of low levels of *Listeria monocytogenes* cells by using a fiber-optic immunosensor. *Applied and Environmental Microbiology* 70:6138-6146.

Ghosh SK, Pal T. 2007. Interparticle coupling effect on the surface plasmon resonance of gold nanoparticles: From theory to applications. *Chemical Reviews* 107:4797-4862.

Glomm WR. 2005. Functionalized gold nanoparticles for applications in bionanotechnology. *Journal of Dispersion Science and Technology* 26:389-414.

Gohji K, Fujimoto N, Komiyama T, Fujii A, Ohkawa J, Kamidono S, Nakajima M. 1996. Elevation of serum levels of matrix metalloproteinase-2 and -3 as new predictors of recurrence in patients with urothelial carcinoma. *Cancer* 78:2379-2387.

Gohji K, Fujimoto N, Fujii A, Komiyama T, Okawa J, Nakajima M. 1996. Prognostic significance of circulating matrix metalloproteinase-2 to tissue inhibitor of metalloproteinases ratio in recurrence of urothelial cancer after complete resection. *Cancer Research* 56:3196-3198.

Gohji K, Fujimoto N, Ohkawa J, Fujii A, Nakajima M. 1998. Imbalance between serum matrix metalloproteinase-2 and its inhibitor as a predictor of recurrence of urothelial cancer. *British Journal of Cancer* 77:650-655.

Goia DV, Matijevic E. 1998. Preparation of monodispersed metal particles. *New Journal of Chemistry* 22:1203-1215.

Goia DV, Matijevic E. 1999. Tailoring the particle size of monodispersed colloidal gold. *Colloids and Surfaces A, Physicochemical and Engineering Aspects* 146:139-152.

Grabar KC, Freeman RG, Hommer MB, Natan MJ. 1995. Preparation and Characterization of Au Colloid Monolayers. *Analytical Chemistry* 67:735-743.

Grabar KC, Brown KR, Keating CD, Stranick SJ, Tang SL, Natan MJ. 1997. Nanoscale characterization of gold colloid monolayers: a comparison of four techniques. *Analytical*

Chemistry 69:471-477.

Graham DL, Ferreira HA, Freitas PP. 2004. Magnetoresistive-based biosensors and biochips. *Trends in Biotechnology* 22:455-462.

Grigioni WF, D'Errico A, Fortunato C, Fiorentino M, Mancini AM, Stetler-Stevenson WG, Sobel ME, Liotta LA, Onisto M, Garbisa S. 1994. Prognosis of gastric carcinoma revealed by interactions between tumour cells and basement membrane. *Modern Pathology* 7:220-225.

Gronewold TM, Glass S, Quandt E, Famulok M. 2005. Monitoring complex formation in the blood-coagulation cascade using aptamer-coated SAW sensors. *Biosensors and Bioelectronics* 20:2044-2052.

Guo S, Wang E. 2007. Synthesis and electrochemical applications of gold nanoparticles. *Analytica Chimica Acta* 598:181-192.

Hainfeld JF, Slatkin DN, Smilowitz HM. 2004. The use of gold nanoparticles to enhance radiotherapy in mice. *Physics in Medicine and Biology* 49:N309-N315.

Halder K, Mathur V, Chugh D, Verma A, Chowdhury S. 2005. Quadruplex-duplex competition in the nuclease hypersensitive element of human c-myc promoter: C to T mutation in C-rich strand enhances duplex association. *Biochemical and Biophysical Research Communications* 327:49-56.

Hanauer M, Pierrat S, Zins I, Lotz A, Sönnichsen C. 2007. Separation of nanoparticles by gel electrophoresis according to size and shape. *Nano Letters* 7:2881-2885.

Hawkes SP, Li H, Taniguchi GT. 2001. Zymography and reverse zymography for detecting MMPs, and TIMPs. *Methods in Molecular Biology* 151:399-410.

Herbst RS, Yano S, Kuniyasu H, Khuri FR, Bucana CD, Guo F, Liu D, Kemp B, Lee JJ, Hong WK, Fidler IJ. 2000. Differential expression of E-cadherin and type IV collagenase genes predicts outcome in patients with stage I non-small cell lung carcinoma. *Clinical Cancer Research* 6:790-797.

Heussen C, Dowdle EB. 1980. Electrophoretic analysis of plasminogen activators in polyacrylamide gels containing sodium dodecyl sulfate and copolymerized substrates. *Analytical Biochemistry* 102:196-202.

Huang CC, Huang YF, Cao Z, Tan W, Chang HT. 2005. Aptamer-modified gold nanoparticles for colorimetric determination of platelet-derived growth factors and their receptors. *Analytical Chemistry* 77:5735-5741.

Huang CC, Chiu SH, Huang YF, Chang HT. 2007. Aptamer-functionalized gold nanoparticles for turn-on light switch detection of platelet-derived growth factor. *Analytical Chemistry* 79:4798-4804.

Hutter E, Fendler JH. 2002. Exploitation of localized surface plasmon resonance. *Advanced Materials* 16:1685-1706.

Inoue T, Yashiro M, Nishimura S, Maeda K, Sawada T, Ogawa Y, Sowa M, Chung KH. 1999. Matrix metalloproteinase-1 expression is a prognostic factor for patients with advanced gastric cancer. *International Journal of Molecular Medicine* 4:73-77.

Ito T, Ito M, Shiozawa J, Naito S, Kanematsu T, Sekine I. 1999. Expression of the MMP-1 in human pancreatic carcinoma: relationship with prognostic factor. *Modern Pathology* 12:669-674.

Jäälinojä J, Herva R, Korpela M, Höyhtyä M, Turpeenniemi-Hujanen T. 2000. Matrix metalloproteinase 2 (MMP-2) immunoreactive protein is associated with poor grade and survival in brain neoplasms. *Journal of Neuro-oncology* 46:81-90.

Jain PK, El-Sayed IH, El-Sayed MA. 2007. Au nanoparticles target cancer. *Nano Today* 2:18-29.

Jena BK, Raj CR. 2008. Optical sensing of biomedically important polyionic drugs using nano-sized gold particles. *Biosensors and Bioelectronics* 23:1285-1290.

Jiang T, Liu R, Huang X, Feng H, Teo W, Xing B. 2009. Colorimetric screening of bacterial enzyme activity and inhibition based on the aggregation of gold nanoparticles. *Chemical Communications* 21:1972-1974.

Jin R, Wu G, Li Z, Mirkin CA, Schatz GC. 2003. What controls the melting properties of DNA-linked gold nanoparticle assemblies? *Journal of the American Chemical Society* 125:1643-1654.

Jones CB, Sane DC, Herrington DM. 2003. Matrix metalloproteinases: a review of their structure and role in acute coronary syndrome. *Cardiovascular Research* 59:812-823.

Kanayama H, Yokota K, Kurokawa Y, Murakami Y, Nishitani M, Kagawa S. 1998. Prognostic values of matrix metalloproteinase-2 and tissue inhibitor of metalloproteinase-2 expression in bladder cancer. *Cancer* 82:1359-1366.

Kanda K, Takahashi M, Murakami Y, Kanayama H, Kagawa S. 2000. The role of the activated form of matrix metalloproteinase-2 in urothelial cancer. *BJU International* 86:553-557.

Kim Y, Johnson RC, Hupp JT. 2001. Gold nanoparticle-based sensing of "spectroscopically silent" heavy metal ions. *Nano Letters* 1:165-167.

Knight AW. 2004. Using yeast to shed light on DNA damaging toxins and irradiation. *The Analyst* 129:866-869.

Koch S, Wolf H, Danapel C, Feller KA. 2000. Optical flow-cell multichannel immunosensor for the detection of biological warfare agents. *Biosensors and Bioelectronics* 14:779-784.

Kodate M, Kasai T, Hashimoto H, Yasumoto K, Iwata Y, Manabe H. 1997. Expression of matrix metalloproteinase (gelatinase) in T1 adenocarcinoma of the lung. *Pathology Iinternational* 47:461-469.

Koivunen E, Arap W, Valtanen H, Rainisalo A, Medina OP, Heikkilä P, Kantor C, Gahmberg CG, Salo T, Konttinen YT, Sorsa T, Ruoslahti E, Pasqualini R. 1999. Tumor targeting with a selective gelatinase inhibitor. *Nature Biotechnology* 17:768-774.

Krieg A, Ruckstuhl T, Laib S, Seeger S. 2004. Real-time detection of polymerase activity using supercritical angle fluorescence. *Journal of Fluorescence* 14:75-78.

Kuittinen O, Savolainen ER, Koistinen P, Turpeenniemi-Hujanen T. 1999. Gelatinase A and B (MMP-2, MMP-9) in leukaemia: MMP-2 may indicate a good prognosis in AML.

Anticancer Research 19:4395-4400.

Kumanan V, Nugen SR, Baeumner AJ, Chang YF. 2009. A biosensor assay for the detection of *Mycobacterium avium* subsp. *paratuberculosis* in fecal samples. *Journal of Veterinary Science* 10:35-42.

Kumar CSSR, Aghasyan M, Modrow H, Doomes E, Henk C, Hormes J. 2004. Synthesis and characterization of S-Au interaction in gold nanoparticle bound polymeric beads. *Journal of Nanoparticle Research* 6:369-376.

Ladd J, Boozer C, Yu Q, Chen S, Homola J, Jiang S. 2004. DNA-directed protein immobilization on mixed self-assembled monolayers via a streptavidin bridge. *Langmuir* 20:8090-8095.

Lai RY, Plaxco KW, Heeger AJ. 2007. Aptamer-based electrochemical detection of picomolar platelet-derived growth factor directly in blood serum. *Analytical Chemistry* 79:229-233.

Leber TM, Balkwill FR. 1997. Zymography: A single-step staining method for quantitation of proteolytic activity on substrate gels. *Analtical Biochemistry* 249:24-28.

Lee AY, Akers KT, Collier M, Li L, Eisen AZ, Seltzer JL. 1997. Intracellular activation of gelatinase A (72-kDa type IV collagenase) by normal fibroblasts. *Proceedings of the National Academy of Sciences of the United States of America* 94:4424-4429.

Lee PW, Peng SF, Su CJ, Mi FL, Chen HL, Wei MC, Lin HJ, Sung HW. 2008. The use of biodegradable polymeric nanoparticles in combination with a low-pressure gene gun for transdermal DNA delivery. *Biomaterials* 29:742-751.

Li CM, Sun CQ, Song S, Choong VE, Maracas G, Zhang XJ. 2005. Impedance labelless detection-based polypyrrole DNA biosensor. *Frontiers in Bioscience* 10:180-186.

Libson AM, Gittis AG, Collier IE, Marmer BL, Goldberg GI, Lattman EE. 1995. Crystal structure of the haemopexin-like C-terminal domain of gelatinase A. *Nature Structural Biology* 2:938-942.

Li J, Chu X, Liu Y, Jiang JH, He Z, Zhang Z, Shen G, Yu RQ. 2005. A colorimetric method for point mutation detection using high-fidelity DNA ligase. *Nucleic Acids Research* 33:e168.

Lidgren L, Lilja O, Krook M, Kriz D. 2006. Automatic fermentation control based on a real-time in situ SIRE® biosensor regulated glucose feed. *Biosensors and Bioelectronics* 21:2010-2013.

Liu J, Lu Y. 2007. Colorimetric Cu^{2+} detection with a ligation DNAzyme and nanoparticles. *Chemical Communications (Cambridge, England)* 14:4872-4874.

Link S, El-Sayed MA. 1999. Size and temperature dependence of the plasmon absorption of colloidal gold nanoparticles. *The Journal of Physical Chemistry B* 103:4212-4217.

Liotta LA, Abe S, Robey PG, Martin GR. 1979. Preferential digestion of basement membrane collagen by an enzyme derived from a metastatic murine tumor. *Proceedings of the National Academy of Sciences of the United States of America* 76:2268-2272.

Liu J, Lu Y. 2003. A colorimetric lead biosensor using DNAzyme-directed assembly of gold nanoparticles. *Journal of the American Chemical Society* 125:6642-6643.

Liu J, Lu Y. 2004. Colorimetric biosensors based on DNAzyme-assembled gold nanoparticles.

Journal of Fluorescence 14:343-354.

Lin YH, Chen SH, Chuang YC, Lu YC, Shen TY, Chang CA and Lin CS. 2008 Disposable amperometric immunosensor for the detection of *Escherichia coli* O157:H7 foodborne pathogen by Au nanoparticles-modified disposable screen printed carbon electrodes. *Biosensors and Bioelectronics* 23:1832-1837.

Lombard C, Saulnier J, Wallach J. 2005. Assays of matrix metalloproteinases (MMPs) activities: a review. *Biochimie* 87:265-272.

Long F, Shi HC, He M, Zhu AN. 2008. Sensitive and rapid detection of 2,4-dicholorophenoxyacetic acid in water samples by using evanescent wave all-fiber immunosensor. *Biosensors and Bioelectronics* 23:1361-1366.

Lu W, Lin L, Jiang L. 2007. Nanogold hollow balls with dendritic surface for hybridization of DNA. *Biosensors and Bioelectronics* 22:1101-1105

Määttä M, Soini Y, Liakka A, Autio-Harmainen H. 2000. Differential expression of matrix metalloproteinase (MMP)-2, MMP-9 and membrane type 1-MMP in hepatocellular and pancreatic adenocarcinoma: implications for tumor progression and clinical prognosis. *Clinical Cancer Research* 6:2726-2734.

Macartney HW, Tschesche H. 1983. Latent and active human polymorphonuclear leukocyte collagenases. Isolation, purification and characterisation. *European Journal of Biochemistry / FEBS* 130:71-78.

Mallya SK, Van Wart HE. 1989. Mechanism of inhibition of human neutrophil collagenase by gold(I) chrysotherapeutic compounds. Interaction at a heavy metal binding site. *The Journal of Biological Chemistry* 264:1594-1601.

Malvern Instruments. Zeta Potential, An Introduction in 30 minutes. Technical notes. on Zetasizer.http://www.nbtc.cornell.edu/facilities/downloads/Zeta%20potential%20-%20An%20introduction%20in%2030%20minutes.pdf

Maxwell DJ, Taylor JR, Nie S. 2002. Self-assembled nanoparticle probes for recognition and detection of biomolecules. *Journal of the American Chemical Society* 124:9606-9612.

Meyer MH, Hartmann M, Krause HJ, Blankenstein G, Mueller-Chorus B, Oster J, Miethe P, Keusgen M. 2007. CRP determination based on a novel magnetic biosensor. *Biosensors and Bioelectronics* 22:973-979.

Michael M, Babic B, Khokha R, Tsao M, Ho J, Pintilie M, Leco K, Chamberlain D, Shepherd FA. 1999. Expression and prognostic significance of metalloproteinases and their tissue inhibitors in patients with small-cell lung cancer. *Journal of Clinical Oncology* 17:1802-1808.

Mirkin CA, Letsinger RL, Mucic RC, Storhoff JJ. 1996. A DNA-based method for rationally assembling nanoparticles into macroscopic materials. *Nature* 382:607-609.

Miyazaki K, Hattori Y, Umenishi F, Yasumitsu H, Umeda M. 1990. Purification and characterization of extracellular matrix-degrading metalloproteinase, Matrin, secreted from rectal carcinoma cell line. *Cancer Research* 50:7758-7764.

Morgunova E, Tuuttila A, Bergmann U, Isupov M, Lindqvist Y, Schneider G, Tryggvason K. 1999. Structure of human pro-matrix metalloproteinase-2: activation mechanism revealed.

Science 284:1667-1670.

Mori M, Mimori K, Shiraishi T, Fujie T, Baba K, Kusumoto H, Haraguchi M, Ueo H, Akiyoshi T. 1997. Analysis of MT1-MMP and MMP2 expression in human gastric cancers. *International Journal of Cancer* 20:316-321.

Murphy G, Bretz U, Baggiolini M, Reynolds JJ. 1980. The latent collagenase and gelatinase of human polymorphonuclear neutrophil leucocytes. *Biochemical Journal* 192:517-525.

Murray GI, Duncan ME, O'Neil P, Melvin WT, Fothergill JE. 1996. Matrix metalloproteinase-1 is associated with poor prognosis in colorectal cancer. *Nature Medicine* 2:461-462.

Murray GI, Duncan ME, O'Neil P, McKay JA, Melvin WT, Fothergill JE. 1998. Matrix metalloproteinase-1 is associated with poor prognosis in oesophageal cancer. *The Journal of Pathology* 185:256-261.

Mwinyihija M, Meharg A, Dawson J, Strachan NJ, Killham K. 2006. An ecotoxicological approach to assessing the impact of tanning industry effluent on river health. *Archives of Environmental Contamination and Toxicology* 50:316-324.

Nagase H, Woessner JF Jr. 1999. Matrix metalloproteinases. *The Journal of Biological Chemistry* 274:21491-21494.

Nakamura H, Karube I. 2003. Current research activity in biosensors. *Analytical and Bioanalytical Chemistry* 377:446-468.

Nakatani HS, dos Santos LV, Pelegrine CP, Gomes STM, Matsushita M, de Souza NE, Visentainer JV. 2005. Biosensor based on xanthine oxidase for monitoring hypoxanthine in fish meat. *American Journal of Biochemistry and Biotechnology* 1:85-89.

Natale Di C, Salimbeni D, Paolesse R, Macagnano A, D'Amico A. 2000. Porphyrins-based opto-electronic nose for volatile compounds detection. *Sensors and Actuators B* 65:220-226.

Nath N, Chilkoti A. 2002. A colorimetric gold nanoparticle sensor to interrogate biomolecularinteractions in real time on a surface. *Analytical Chemistry* 74:504-510.

Nath N, Chilkoti A. 2004. Label free colorimetric biosensing using nanoparticles. *Journal of Fluorescence* 14:377-389.

Netzel-Arnett S, Mallya SK, Nagase H, Birkedal-Hansen H, Van Wart HE. 1991. Continuously recording fluorescent assays optimized for five human matrix metalloproteinases. *Analytical Biochemistry* 195:86-92.

Nikkola J, Vihinen P, Vlaykova T, Hahka-Kemppinen M, Kähäri VM, Pyrhönen S. 2002. High expression levels of collagenase-1 and stromelysin-1 correlate with shorter disease-free survival in human metastatic melanoma. *International Journal of Cancer* 97:432-438.

Oberg A, Höyhtyä M, Tavelin B, Stenling R, Lindmark G. 2000. Limited value of preoperative serum analyses of matrix metalloproteinases (MMP-2, MMP-9) and tissue inhibitors of matrix metalloproteinases (TIMP-1, TIMP-2) in colorectal cancer. *Anticancer Research* 20:1085–1091.

Oh E, Lee D, Kim YP- Cha SY, Oh DB, Kang HA, Kim J, Kim HS. 2006. Nanoparticle-based

energy transfer for rapid and simple eetection of protein glycosylation. *Angewandte Chemie* 45:7959-7963.

Oh E, Hong MY, Lee D, Nam SH, Yoon HC, Kim HS. 2005. Inhibition assay of biomolecules based on fluorescence resonance energy transfer (FRET) between quantum dots and gold nanoparticles. *Journal of the American Chemical Society* 127:3270-3271.

Okada Y, Morodomi T, Enghild JJ, Suzuki K, Yasui A, Nakanishi I, Salvesen G, Nagase H. 1990. Matrix metalloproteinase 2 from human rheumatoid synovial fibroblasts. Purification and activation of the precursor and enzymic properties. *European Journal of Biochemistry / FEBS* 194:721-730.

Okitsu K, Yue A, Tanabe S, Matsumoto H, Yobiko Y. 2001. Formation of colloidal gold nanoparticles in an ultrasonic field: Control of rate of gold(III) reduction and size of formed gold particles. *Langmuir* 17:7717-7720.

Opitz L, Zimmermann A, Lehmann S, Genzel Y, Lübben H, Reichl U, Wolff MW. 2008. Capture of cell culture-derived influenza virus by lectins: Strain independent, but host cell dependent. *Journal of Virological Methods* 154:61-68.

Palmisano F, Rizzi R, Centonze D, Zambonin PG. 2000. Simultaneous monitoringof glucose and lactose by an interference and cross-talk free dual electrode amperometric biosensor based on electropolymerized thin films. *Biosensors and Bioelectronics* 15:531-539.

Park SJ, Taton TA, Mirkin CA. 2002. Array-based electrical detection of DNA with nanoparticle probes. *Science* 295:1503-1506.

Pashley RM, Karaman ME. 2005. Van der Waals forces and colloid stability. *Applied colloid and Surface Chemistry* 127-151.

Passlick B, Sienel W, Seen-Hibler R, Wöckel W, Thetter O, Mutschler W, Pantel K. 2000. Overexpression of matrix metalloproteinase 2 predicts unfavourable outcome in early-stage non-small cell lung cancer. *Clinical Cancer Research* 6:3944-3948.

Patel N G, Meier S, Cammann K, Chemnitius G C. 2001. Screen-printed biosensors using different alcohol oxidases. *Sensors and Actuators B* 75: 101-110.

Pellegrino T, Kudera S, Liedl T, Muñoz Javier A, Manna L, Parak WJ. 2005. On the development of colloidal nanoparticles towards multifunctional structures and their possible use for biological applications. *Small* 1:48-63.

Persoons A, Verbiest T. 2006. An experimental study on the preparation of gold nanoparticles and their properties. *Katholieke universiteit Leuven.* https://repository.libis.kuleuven.be/dspace/bitstream/1979/254/2/thesis_finaal.pdf

Phelps MR, Hobbs JB, Kilburn DG, Turner RF. 1995. An autoclavable glucose biosensor for microbial fermentation monitoring and control. *Biotechnology and Bioengineering* 46:514-524.

Rao CNR, Cheethama A.. 2001. Science and technology of nanomaterials: current status and future prospects. *Journal of Materials Chemistry* 11: 2887-2894.

Ray PC, Fortner A, Darbha GK. 2006. Gold nanoparticle based FRET asssay for the detection of DNA cleavage. *The Journal of Physical Chemistry. B* 110:20745-20748.

Rasmussena LD, Sùrensena SJ, Turnerb RR, Barkay T. 2000. Application of a mer-lux biosensor for estimating bioavailable mercury in soil. *Soil Biology and Biochemistry* 32:639-646.

Ratnikov BI, Deryugina EI, Strongin AY. 2002. Gelatin zymography and substrate cleavage assays of matrix metalloproteinase-2 in breast carcinoma cells overexpressing membrane type-1 matrix metalloproteinase. *Laboratory Investigation* 82:1583-1590.

Riedel F, Götte K, Schwalb J, Bergler W, Hörmann K. 2000. Expression of 92-kDa type IV collagenase correlates with angiogenic markers and poor survival in head and neck squamous cell carcinoma. *International Journal of Oncology*17:1099-1105.

Rodriguez JA, Dvorak J, Jirsak T, Liu G, Hrbek J, Aray Y, Gonzalez C. 2003. Coverage effects and the nature of the metal-sulfur bond in S/Au(111): High-resolution photoemission and density-functional studies. *Journal of the American Chemical Society* 125:276-285.

Roeb E, Matern S. 2001. Matrix metalloproteinases: Promoters of tumor invasion and metastasis - A review with focus on gastrointestinal tumors. *Zeitschrift für Gastroenterologie* 39:807-813.

Rojo J, Díaz V, de la Fuente JM, Segura I, Barrientos AG, Riese HH, Bernad A, Penadés S. 2004. Gold glyconanoparticles as new tools in antiadhesive therapy. *Chembiochem* 5:291-297.

Rosi NL, Mirkin CA. 2005. Nanostructures in biodiagnostics. *Chemical Reviews* 105:1547-1562.

Sakakibara M, Koizumi S, Saikawa Y, Wada H, Ichihara T, Sato H, Horita S, Mugishima H, Kaneko Y, Koike K. 1999. Membrane-type matrix metalloproteinase-1 expression and activation of gelatinase A as prognostic markers in advanced pediatric neuroblastoma. *Cancer* 85:231-239.

Salem AK, Searson PC, Leong KW. 2003. Multifunctional nanorods for gene delivery. *Nature Materials* 2:668-671.

Sapsford KE, Berti L, Medintz IL. 2006. Materials for fluorescence resonance energy transfer analysis: Beyond traditional donor-acceptor combinations. *Angewandte Chemie* 45:4562-4589.

Saraiva SM, de Oliveira JF. 2002. Control of particle size in the preparation of colloidal gold. *Journal of Dispersion Science and Technology* 23:837-844.

Sato K, Hosokawa K, Maeda M. 2003. Rapid aggregation of gold nanoparticles induced by non-cross-linking DNA hybridization. *Journal of the American Chemical Society* 125:8102-8103.

Schultz DA. 2003. Plasmon resonant particles for biological detection. *Current Opinion in Biotechnology* 14:13-22

Schulz R. 2007. Intracellular targets of matrix metalloproteinase-2 in cardiac disease: rationale and therapeutic approaches. *Annual Review of Pharmacology and Toxicology* 47:211-242.

Sellers A, Cartwright E, Murphy G, Reynolds JJ. 1977. Evidence that latent collagenases are

enzyme-inhibitor complexes. *The Biochemical Journal* 163:303-307.

Sellers A, Reynolds JJ, Meikle MC. 1978. Neutral metallo-proteinases of rabbit bone. Separation in latent forms of distinct enzymes that when activated degrade collagen, gelatin and proteoglycans. *The Biochemical Journal* 171:493-496.

Shaw DJ. 1980. Introduction to colloid and surface chemistry. *London: Butterworths*, 3rd edition.

Sier CF, Kubben FJ, Ganesh S, Heerding MM, Griffioen G, Hanemaaijer R, van Krieken JH, Lamers CB, Verspaget HW. 1996. Tissue levels of matrix metalloproteinases MMP-2 and MMP-9 are related to the overall survival of patients with gastric carcinoma. *British Journal of Cancer* 74:413-417.

Slocik JM, Zabinski JS Jr, Phillips DM, Naik RR. 2008. Colorimetric response of peptide-functionalized gold nanoparticles to metal ions. *Small* 4:548-551.

Smutok O, Ngounou B, Pavlishko H, Gayda G, Gonchar M, Schuhmann W. 2006. A reagentless bienzyme amperometric biosensor based on alcohol oxidase/peroxidase and an Os-complex modified electrodeposition paint. *Sensors and Actuators B* 113: 590-598.

Snoek-van Beurden PA, Von den Hoff JW. 2005. Zymographic techniques for the analysis of matrix metalloproteinases and their inhibitors. *BioTechniques* 38:73-83.

Sönnichsen C, Franzl T, Wilk T, Plessen G von, and Feldmann J. 2002. Plasmon resonances in large noble-metal clusters. *New Journal of Physics* 4:931-938.

Sperling RA, Rivera Gil P, Zhang F, Zanella M, Parak WJ. 2008. Biological applications of gold nanoparticles. *Chemical Society Reviews* 37:1896-1908.

Springman EB, Angleton EL, Birkedal-Hansen H, Van Wart HE. 1990. Multiple modes of activation of latent human fibroblast collagenase: evidence for the role of a Cys73 active-site zinc complex in latency and a "cysteine switch" mechanism for activation. *Proceedings of the National Academy of Sciences of the United States of America* 87:364-368.

Stawowy P, Margeta C, Kallisch H, Seidah NG, Chrétien M, Fleck E, Graf K. 2004. Regulation of matrix metalloproteinase MT1-MMP/MMP-2 in cardiac fibroblasts by TGF-beta1 involves furin-convertase. *Cardiovascular Research* 63:87-97.

Stefanidakis M, Koivunen E. 2006. Cell-surface association between matrix metalloproteinases and integrins: role of the complexes in leukocyte migration and cancer progression. *Blood* 108:1441-1450.

Stricklin GP, Jeffrey JJ, Roswit WT, Eisen AZ. 1983. Human skin fibroblast procollagenase: mechanisms of activation by organomercurials and trypsin. *Biochemistry* 22:61-68.

Su KH, Wei QH, Zhang X, Mock JJ, Smith DR, Schultz S. 2003. Interparticle coupling effects on plasmon resonances of nanogold particles. *Nano Letters* 3:1087-1090.

Sullivan MMO, Green JJ, Przybycien TM. 2003. Development of a novel gene delivery scaffold utilizing colloidal gold-polyethylenimine conjugates for DNA condensation. *Gene Therapy* 10:1882-1890.

Sun Y and Xia Y. 2003. Gold and silver nanoparticles: a class of chromophores with colors tunable in the range from 400 to 750 nm. *The Analyst* 128:686-691.

Talvensaari-Mattila A, Pääkkö P, Höyhtyä M, Blanco-Sequeiros G, Turpeenniemi-Hujanen T. 1998. Matrix metalloproteinase-2 immunoreactive protein: a marker of aggressiveness in breast carcinoma. *Cancer* 83:1153-1162.

Tan HY, Loke WK, Tan YT, Nguyen NT. 2008. A lab-on-a-chip for detection of nerve agent sarin in blood. *Lab on a Chip* 8:885-891.

Tang D, Yuan R, Chai Y. 2007. Biochemical and immunochemical characterization of the antigen-antibody reaction on a non-toxic biomimetic interface immobilized red blood cells of crucian carp and gold nanoparticles. *Biosensors and Bioelectronics* 22:1116-1120.

Tischer BK, Schumacher D, Beer M, Beyer J, Teifke JP, Osterrieder K, Wink K, Zelnik V, Fehler F, Osterrieder N. 2002. A DNA vaccine containing an infectious Marek's disease virus genome can confer protection against tumorigenic Marek's disease in chickens. *The Journal of General Virology* 83:2367-2376.

Tsai CS, Yu TB, Chen CT. 2005. Gold nanoparticle-based competitive colorimetric assay for detection of protein-protein interactions. *Chemical Communications* 14:4273-4275.

Turkevich J. 1985. Colloidal gold. Part 1. *Gold Bulletin* 18:86-91.

Vaiopoulou E, Melidis P, Kampragou E, Aivasidis A. 2005. On-line load monitoring of wastewaters with a respirographic microbial sensor. *Biosensors and Bioelectronics* 21:365-371.

Väisänen A, Kallioinen M, Taskinen PJ, Turpeenniemi-Hujanen T. 1998. Prognostic value of MMP-2 immunoreactive protein (72 kD type IV collagenase) in primary skin melanoma. *The Journal of Pathology* 186:51-58.

Van Wart HE, Birkedal-Hansen H. 1990. The cysteine switch: a principle of regulation of metalloproteinase activity with potential applicability to the entire matrix metalloproteinase gene family. *Proceedings of the National Academy of Sciences of the United States of America* 87:5578-5582.

Vo-Dinh T, Cullum B. 2000. Biosensors and biochips: advances in biological and medical diagnostics. *Fresenius' Journal of Analytical Chemistry* 366:540-551.

Vihinen P, Kähäri VM. 2002. Matrix metalloproteinases in cancer: prognostic markers and therapeutic targets. *International journal of cancer* 99:157-166.

Wallon UM, Overall CM. 1997. The hemopexin-like domain (C domain) of human gelatinase A (matrix metalloproteinase-2) requires Ca^{2+} for fibronectin and heparin binding. Binding properties of recombinant gelatinase A C domain to extracellular matrix and basement membrane components. *The Journal of Biological Chemistry* 272:7473-7481.

Wang M, Gu X, Zhang G, Zhang D, Zhu D. 2009. Continuous colorimetric assay for acetylcholinesterase and inhibitor screening with gold nanoparticles. *Langmuir* 25:2504-2507.

Wang Y, Li D, Ren W, Liu Z, Dong S, Wang E. 2008. Ultrasensitive colorimetric detection of protein by aptamer-Au nanoparticles conjugates based on a dot-blot assay. *Chemical Communications (Cambridge, England)* 22:2520-2522.

Wang Z, Lévy R, Fernig DG, Brust M. 2006. Kinase-catalyzed modification of gold nanoparticles: a new approach to colorimetric kinase activity screening. *Journal of the*

American Chemical Society 128:2214-2215.

Weiss SJ, Peppin G, Ortiz X, Ragsdale C, Test ST. 1985. Oxidative autoactivation of latent collagenase by human neutrophils. *Science* 227:747-749.

Westerlund A, Apaja-Sarkkinen M, Höyhtyä M, Puistola U, Turpeenniemi-Hujanen T. 1999. Gelatinase A-immunoreactive protein in ovarian lesions-prognostic value in epithelial ovarian cancer. *Gynecologic Oncology* 75:91-98.

Whyman R. 1996. Gold nanoparticles. A renaissance in gold chemistry. *Gold Bulletin* 29:11-15.

Woessner JF Jr. 1995. Quantification of matrix metalloproteinases in tissue samples. *Methods in Enzymology* 248:510-528.

Wu BY, Hou SH, Yin F, Li J, Zhao ZX, Huang JD, Chen Q. 2007. Amperometric glucose biosensor based on layer-by-layer assembly of multilayer films composed of chitosan, gold nanoparticles and glucose oxidase modified Pt electrode. *Biosensors and Bioelectronics* 22:838-844.

Wu VCH, Chen SH and Lin CS. 2007. Real-time detection of *Escherichia coli* O157:H7 sequences using a circulating-flow system of quartz crystal microbalance. *Biosensors and Bioelectronics* 22: 2967-2975.

Wu X, Choi MMF, Xiao D. 2000. A glucose biosensor with enzyme-entrapped sol–gel and an oxygen-sensitive optode membrane. *Analyst* 125:157-162.

Xiao Y, Ju HX, Chen HY. 1999. Hydrogen peroxide sensor based on horseradish peroxidase-labeled Au colloids immobilized on gold electrode surface by cysteamine monolayer. *Analytica Chimica Acta* 391:73-82.

Xiao Y, Patolsky F, Katz E, Hainfeld JF, Willner I. 2003. "Plugging into enzymes": Nanowiring of redox enzymes by a gold nanoparticle. *Science* 299:1877-1881.

Xu X, Han MS, Mirkin CA. 2007. A gold-nanoparticle-based real-time colorimetric screening method for endonuclease activity and inhibition. *Angewandte Chemie* 46:3468-3470.

Yamada A, Uegaki A, Nakamura T, Ogawa K. 2000. ONO-4817, an orally active matrix metalloproteinase inhibitor, prevents lipopolysaccharide-induced proteoglycan release from the joint cartilage in guinea pigs. *Inflammation Research* 49:144-146.

Yamamoto A, Yano S, Shiraga M, Ogawa H, Goto H, Miki T, Zhang H, Sone S. 2003. A third-generation matrix metalloproteinase (MMP) inhibitor (ONO-4817) combined with docetaxel suppresses progression of lung micrometastasis of MMP-expressing tumor cells in nude mice. *International Journal of Cancer* 103:822-828

Yamamoto H, Itoh F, Iku S, Adachi Y, Fukushima H, Sasaki S, Mukaiya M, Hirata K, Imai K. 2001. Expression of matrix metalloproteinases and tissue inhibitors of metalloproteinases in human pancreatic adenocarcinomas: clinicopathologic and prognostic significance of matrilysin expression. *Journal of Clinical Oncology* 15:1118-1127

Yamashita K, Mori M, Shiraishi T, Shibuta K, Sugimachi K. 2000. Clinical significance of atrix metalloproteinase-7 expression in esophageal carcinoma. *Clinical Cancer Research* 6:1169-1174.

Yamashita K, Mori M, Kataoka A, Inoue H, Sugimachi K. 2001. The clinical significance of MMP-1 expression in eosophageal carcinoma. *British Journal of Cancer* 84:276-282.

Yang Q, Wang S, Fan P, Wang L, Di Y, Lin K, Xiao FS. 2005. pH-Responsive Carrier System Based on Carboxylic Acid Modified Mesoporous Silica and Polyelectrolyte for Drug Delivery. *Chemistry of Materials* 17:5999-6003.

Ylisirniö S, Höyhtyä M, Turpeenniemi-Hujanen T. 2000. Serum matrix metalloproteinases-2, -9 and tissue inhibitors of metalloproteinases-1, -2 in lung cancer-TIMP-1 as a prognostic marker. *Anticancer Research* 20:1311-1316.

Yoshizaki T, Maruyama Y, Sato H, Furukawa M. 2001. Expression of tissue inhibitor of matrix metalloproteinase-2 correlates with activation of matrix metalloproteinase-2 and predicts poor prognosis in tongue squamous cell carcinoma. *International Journal of Cancer* 95:44-50

Yuan J, Oliver R, Li J, Lee J, Aguilar M, Wu Y. 2007. Sensitivity enhancement of SPR assay of progesterone based on mixed self-assembled monolayers using nanogold particles. *Biosensors and Bioelectronics* 23:144-148.

Zeng ZS, Huang Y, Cohen AM, Guillem JG. 1996. Prediction of colorectal cancer relapse and survival via tissue RNA levels of matrix metalloproteinase- 9. *Journal of Clinical Oncology* 14:3133-3140.

Zeta-Meter, Inc. 1993. "Everything you want to know about coagulation & flocculation". http://www.mtec.or.th/labs/powder/docs/coagulation.pdf

Zhang Q, Huang Y, Zhao R, Liu G, Chen Y. 2008. Determining binding sites of drugs on human serum albumin using FIA-QCM. *Biosensors and Bioelectronics* 24:48-54.

Zhao W, Chiuman W, Lam JC, Brook MA, Li Y. 2007. Simple and rapid colorimetric enzyme sensing assays using non-crosslinking gold nanoparticle aggregation. *Chemical Communications (Cambridge, England)* 36:3729-3371.

Zhao W, Brook MA, Li Y. 2008. Design of gold nanoparticle-based colorimetric biosensing assays. *Chembiochem* 9:2363-2371.

Zhao W, Chiuman W, Lam JC, McManus SA, Chen W, Cui Y, Pelton R, Brook MA, Li Y. 2008. DNA aptamer folding on gold nanoparticles: from colloid chemistry to biosensors. *Journal of the American Chemical Society* 130:3610-3618.

Zhu X, Yang Q, Huang J, Suzuki I, Li G. 2008. Colorimetric study of the interaction between gold nanoparticles and a series of amino acids. *Journal of Nanoscience and Nanotechnology* 8:353-335.

Zucker S, Lysik RM, Zarrabi MH, Moll U. 1993. M(r) 92,000 type IV collagenase is increased in plasma of patients with colon cancer and breast cancer. *Cancer Research* 53:140-146.

Table 1-1. Common transducers used in biosensing systems

Category	Description
Amperometric transducers	Amperometric devices detect changes in current as constant potential measures currents generated when electrons are exchanged between a biological system and an electrode.
Conductive transducers	Conductimetric devices detect changes in conductivity between two electrodes.
Capacitive transducers	When the biorecognition reaction causes a change in the dielectric constant of the medium in the vicinity of the bioreceptor, capacitance measurement method can be used as a transducer.
Optical can be subdivided into two modes according to the optical configuration	Optical biosensors correlate changes in concentration, mass, or number of molecules to direct changes in the characteristics of light. For this method to work, one of the reactants or products of the biorecognition reaction has to link to colorimetric, fluorescent or luminescent indicator molecules. Usually, an optical fiber is used for guiding the light signals from the source to the detector.
Extrinsic optical transducers	In the extrinsic mode, the incident wave is not directed through the bulk sample, but propagates along a wave guide and interacts with the sample at the surface within the evanescent field. Other surface methods of optical detection of biological recognition are based on modulation of the field excited at the interface between different materials due to incident light.
Intrinsic optical transducers	In the intrinsic mode, the incident light passes through the sample and interacts directly with the sample.
Piezoelectric transducers	These devices detect changes in mass.
Potentiometric transducers	Electrodes detect changes in potential at constant current.
Thermal transducers	These devices measure changes in temperature.

[http://www.emeraldinsight.com/fig/0870170202001.png]

Table 1-2. The applications of biosensors

Application	Target	Biorecognition element	Transduction	Reference
Clinical diagnosis and biomedicine				
Acute myocardial infarction	Cardiac troponin T	Enzyme	Optical (SPR)	Dutra et al., 2007
Atherosclerosis, fibrosis, malignant diseases	Platelet-derived growth factor	Aptamer	Electrochemical	Lai et al., 2007
Breast cancer	*BRCA1* gene	DNA	Electrochemical	Castañeda et al, 2007
Inflammation Cardiovascular diseases	c-reactive protein	Enzyme	Magnetic	Meyer et al. 2007
Progesterone	Progesterone	Enzyme	Optical (SPR)	Yuan et al, 2007
Farm, garden and veterinary analysis				
Bioavailable mercury in soil	Bioavailable mercury	Bacterial	Optical	Rasmussena et al, 2000
Influenza virus	virus	Lectin	Optical	Opitz et al, 2008
Mycobacterium avium subsp. *paratuberculosis*	IS*900* gene	DNA	Optical	Kumanan et al, 2009
Pesticide	Carbaryl pesticide	Enzyme	Electrochemical	Du et al, 2007
Process control: fermentation control and analysis				
Alcohol fermentation	Glycerol	Enzyme	Electrochemical	Compagnone et al, 1998
Alcohol fermentation	Alcohol	Enzyme	Electrochemical	Patel et al, 2001
Lactose fermentation	Lactose	Enzyme	Electrochemical	Ferreira et al, 2003
Microbial fermentation	Glucose	Enzyme	Electrochemical	Phelps et al, 1995
Yeast fermentation	Glucose	Enzyme	Electrochemical	Lidgren et al, 2006
Food and drink production and analysis				
Beverages	Glucose and glutamate	Enzyme	Optical	Wu et al, 2000
Fish	Hypoxanthine	Enzyme	Electrochemical	Nakatani et al, 2005
Tomato juice	glucose and lactate	Enzyme	Electrochemical	Palmisano et al, 2000
Wine	Ethanol	Enzyme	Electrochemical	Smutok et al, 2006

Continued

Application	Target	Biorecognition element	Transduction	Reference
Microbiology: bacterial and viral analysis				
Campylobacter jejuni.	Bacteria	Enzyme	Electrochemical	Che et al, 2001
E. coli O157:H7	Bacteria	Enzyme	Electrochemical	Lin et al, 2008
E. coli O157:H7	DNA sequences	DNA	Piezoelectric (QCM)	Wu et al, 2007; Chen et al, 2008
L.monocytogenes	Bacteria	Enzyme	Optical	Geng et al, 2004
Pharmaceutical and drug analysis				
Drug-binding site	Drug	Protein	Piezoelectric (QCM)	Zhang et al, 2008
Discovery of antibiotics	Moenomycin derivatives	Enzyme	Optical	Cheng et al, 2008
Industrial effluent control				
Monitoring of wastewaters	CO_2 monitor	Microbial	Optical	Vaiopoulou et al, 2005
Water quality	Heavy metals	Microbial	Optical	Mwinyihija et al, 2006
Pollution control and monitoring				
Herbicide	2,4-dichlorophenoxyacetic acid	Enzyme	Optical	Long et al, 2008
Water quality	Heavy metals	Microbial	Optical	Mwinyihija et al, 2006
Mining, industrial and toxic gases				
Volatile organic compounds (VOC) detection	VOC	Fluorescent dyes	Optical	Dickinson et al, 1996
Volatile organic compounds (VOC) detection	VOC	Metalloporphyrines	Optical	Natale et al, 2000
Military applications				
Biological warfare agents	Bacteria and virus agent	Enzyme	Optical	Koch et al, 2000
Chemical warfare agents	Sarin	Enzyme	Optical	Tan et al, 2008

Table 1-3. The applications of AuNPs

Application	Method	Assistant technology	Reference
Biosensor			
Detection of DNA	Colorimetric detection	Self-assembly	Mirkin et al., 1996
Detection of metal ion	Colorimetric detection	Aptamers	Liu and Lu, 2007
Detection of enzyme activity and screening of inhibitors	Colorimetric detection	Self-assembly	Jiang et al., 2009
Protein-protein interaction	Colorimetric detection	Self-assembly	Tsai et al., 2005
Detection of DNA	Fluorescence resonance energy transfer (FRET)		Maxwell et al., 2002
Protein-protein interaction	Fluorescence resonance energy transfer (FRET)		Oh et al., 2005
Detection of glucose	Elechemical	AuNPs modified with oxidase	Xiao et al., 2003
Detection of hydrogen peroxide	Elechemical	AuNPs immobilized on the electrode surface	Xiao et al., 1999
Drug delivery system			
Drug delivery	Endocytosis		Rojo et al., 2004
Gene delivery	Endocytosis		Sullivan et al., 2003
Gene delivery	Gene gun		Lee et al., 2008
Bioimaging			
Cells migrating	Endocytosis		Albrecht-Buehler, 1979
Visualization of microtubules in plants	Immuno-gold staining		Faulk and Taylor, 1971

Table 1-4. Prognostic value of mmps in cancer

Cancer type	MMP	Expression level	Impact on survival	Reference
Acute myeloid leukaemia	MMP-2	Positive	Good prognosis	Kuittinen et al., 1999
Brain tumours	MMP-2	Positive	Poor survival	Jäälinojä et al., 2000
Breast carcinoma	MMP-2	Positive	Poor survival	Talvensaari-Mattila et al, 1998
	MMP-11	High	Poor survival & DFS	Chenard et al, 1996
Cervical carcinoma	MMP-2	High	Poor prognosis	Davidson et al, 1999
	MMP-1	Positive	Poor prognosis	Murray et al, 1996
Colorectal carcinoma	MMP-2	High	Poor survival	Oberg et al, 2000
	MMP-9	High	Poor survival & DFS	Zeng et al, 1996
	MMP-9	High	Poor prognosis	Zucker et al, 1993
	MMP-1	Positive	Poor prognosis	Inoue et al, 1999
	MMP-2	Positive	Poor prognosis	Grigioni et al, 1994
Gastric carcinoma	MMP-2, -9	High	Poor survival	Sier et al, 1996
	MMP-2	High	Poor prognosis	Allgayer et al, 1998
	MT1-MMP		Poor prognosis	Mori et al, 1997
	MT1-MMP	Positive	Poor prognosis	Bando et al, 1998
Hepatocellular carcinoma	MT1-MMP	High	Poor prognosis	Määttä et al, 2000
Head and neck squamous cell carcinoma	MMP-9	Positive	Poor survival	Riedel et al, 2000
Lung adenoca	MMP-2, -9	High	Poor prognosis	Kodate et al, 1997
Lung carcinoma	MMP-9	High	Poor survival	Ylisirniö et al, 2000
Nonsmall cell lung cancer	MMP-2	High	Poor prognosis	Passlick et al, 2000
	MMP-2, -9	Low	Longer DFS	Herbst et al, 2000

Continued

Cancer type	MMP	Expression level	Impact on survival	Reference
	MMP-9	Positive	Poor prognosis	Cox et al, 2000
Small cell lung cancer	MMP-3, -11, MT1-MMP	Positive	Poor survival	Michael et al, 1999
Melanoma (Skin)	MMP-2	High	Better/poor surviva	Väisänen et al, 1998
Melanoma (Metastatic)	MMP-1, -3	High	Poor DFS	Nikkola et al, 2002
Neuroblastoma	MT1-MMP	High	Poor survival	Sakakibara et al, 1999
	MMP-1	Positive	Poor survival	Murray et al, 1998
Oesophageal carcinoma	MMP-1	High	Poor prognosis	Yamashita et al, 2001
	MMP-7	High	Poor prognosis	Yamashita et al, 2000
	MMP-13	High	Poor prognosis	Etoh et al, 2000
Ovarian carcinoma	MMP-2	High	Poor prognosis	Westerlund et al, 1999
	MMP-9	High	Poor prognosis	Davidson et al, 1999
Pancreatic adenoca	MMP-1	Positive	Poor prognosis	Ito et al, 1999
	MMP-7	Positive	Poor survival	Yamamoto et al, 2001
Tongue SCC	MMP-2, MT1-MMP	Positive	Poor prognosis	Yoshizaki et al, 2001
	MMP-2, MT1-MMP	High	Poor survival	Kanayama et al, 1998
Urothelial carcinoma	MMP-2, -3	High	Poor DFS	Gohji et al, 1996
	MMP-2	High	Poor DFS	Gohji et al, 1996; Kanda et al, 2000
	MMP-2	High	prognosis	Gohji et al, 1998

DFS, disease-free survival; DSS, disease-specific survival

Table 1-5. Classification and nomenclature of MMPs

Group	MMP	MMajor substrates	Activators	Inhibitors
Collagenases				
Collagenases 1	MMP–1	Collagen I, II, III, VII, VIII, X, aggregan, serpins, 2-macroglobulin	MMP-3, -7, -10, plasmin, kallikrein, chymase	TIMP–1, –2, –3, –4
Collagenases 2	MMP–8	Collagen I, II, III, aggregan, serpins, 2-macroglobuli	MMP–3,–10, Plasmin	TIMP–1, –2
Collagenases 3	MMP–13	Collagen I, II, III, IV, IX, X, XIV, gelatin, fibronectin, laminin, fibrillin, osteonectin, serpins, large tenascin aggrecan	MMP–2, –3, –10, –14, –15, plasmin	
Collagenases 4 (*Xenopus*)	MMP–18	Collagen	ND	
Stromelysins				
Stromelysin 1	MMP–3	Collagen IV, V, IX, X, fibronectin, elastin, gelatin, laminin, aggrecan, nidoge fibrillin*, osteonectin*, 1-proteinase inhibitor *, myelin basic protein*, osteopontin, E-cadherin	Plasmin, kallikrein, chymase, tryptase	TIMP–1, –2, –3, –4
Stromelysins 2	MMP–10	As MMP-3, except *	Elastase, cathepsin G	TIMP–1, –2,
Stromelysins 3	MMP–11	Serine proteinase inhibitors, 1-proteinase inhibitor	Furin	TIMP–1, –2,
Gelatinases				
Gelatinase A	MMP–2	Gelatin, collagen I, IV, V, VII, X, fibronectin, tenascin, fibrillin, osteonectin, Monocyte chemoattractant protein 3	MMP–1, –7, –13, –14, –15, –16, –17, –24, –25, trypsin	TIMP–1, –2, –3, –4
Gelatinase B	MMP–9	Gelatin, collagen IV, V, VII, XI, XIV, elastin, fibrillin, osteonectin 2	MMP-2, -3, 7, -13, plasmin, trypsin, chymotrypsin, cathepsin G	TIMP–1, –2, –3, –4
Membrane-type MMPs				
Transmembrane				
MT1–MMP	MMP–14	Collagen I, II, III, gelatin, fibronectin, laminin, vitronectin, aggrecan, tenasci nidogen, perlecan, fibrillin, 1-proteinase inhibitor, 2-macroglobulin, fibrin	Plasmin, furin	TIMP–2, –3
MT2–MMP	MMP–15	fibronectin, laminin, aggrecan, tenascin, nidogen, perlecan	ND	
MT3–MMP	MMP–16	Collagen III, fibronectin, gelatin, casein, cartilage proteoglycans, laminin-1, 2-macroglobulin	ND	
MT5–MMP	MMP–24	Proteoglycans	ND	

Continued

Group	MMP	MMajor substrates	Activators	Inhibitors
GPIanchor				
MT4–MMP	MMP–17	Fibrin, fibrinogen, TNF precursor	ND	
MT6–MMP	MMP–25	Collagen IV, gelatin, fibronectin, fibrin	ND	
Matrilysins				
Matrilysin 1; Pump–1	MMP–7	Elastin, fibronectin, laminin, nidogen, collagen IV, tenascin, versican, 1-proteinase inhibitor, O E-cadherin, TNF-	MMP–2, -3 –10, plasmin	TIMP–1, –2, –4
Matrilysin 2	MMP–26	Gelatin, 1-proteinase inhibitor, synthetic MMP-substrates, TACE-substrate	ND	
Others				
Macrophage; elastase	MMP–12	Collagen IV, gelatin, fibronectin, laminin, vitronectin, elastin, fibrillin, 1-PI, myelin basic protein, apolipoprotein A	ND	TIMP–1, –2
No trivial name	MMP–19	Gelatin, aggrecan, cartilage oligomeric matrix protein, collagen IV, laminin, nidogen, large tenas	Trupsin	
Enamelysin	MMP–20	Amelogenin, aggrecan, cartilage oligomeric matrix protein	ND	
XMMP (*Xenopus*)	MMP–21		ND	
CA–MMP	MMP–23	McaPLGLDpaARNh2 (synthetic MMP substrate)	ND	
CMMP (*Gallus*)	MMP–27	Collagen I	ND	
Epilysin	MMP–28	Casein	ND	

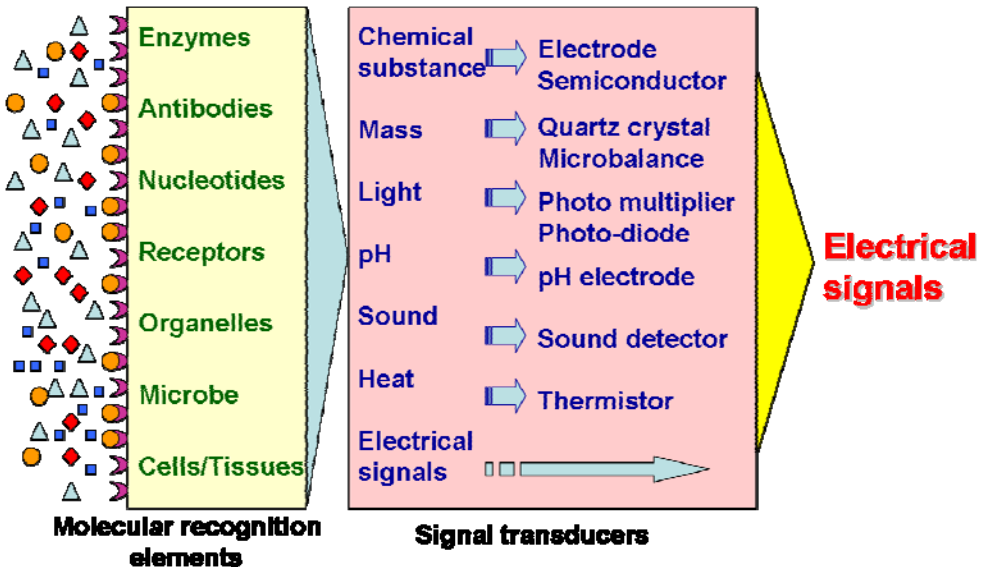

Figure 1-1. The principle of biosensing systems. Biosensors are analytical tools combining a biochemical recognition component with a physical transducer. The biological sensing element can be an enzyme, antibody, DNA sequence, or even microorganism. The biochemical component serves to selectively catalyze a reaction or facilitate a binding event. The selectivity of the biochemical recognition event allows for the operation of biosensors in a complex sample matrix, i.e., a body fluid. The transducer can take many forms depending upon the parameters being measured - electrochemical, optical, mass and light changes are the most common. The transducer converts the biochemical event into a measurable signal, thus providing the means for detecting it. Measurable events range from spectral changes, which are due to production or consumption of an enzymatic reaction's product/substrate, to mass change upon biochemical complex. The transducer output electric signal in the monitor real time.

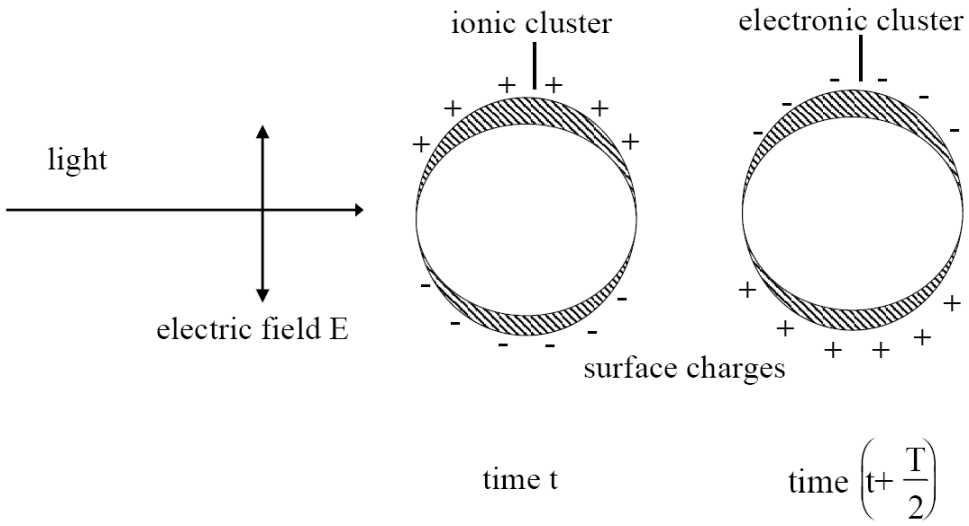

Figure 1-2. Schematic presentation of the surface plasmon resonance. A schematic representation illustrating the optical response of a metal colloid to an electric field (an incident light wave) leading to a dipolar surface plasmon. The negative charges (the conduction electrons) move under the influence of the external field. The phenomenon induces surface electron oscillation of metal colloid is so-called surface plasmon resonance (SPR).

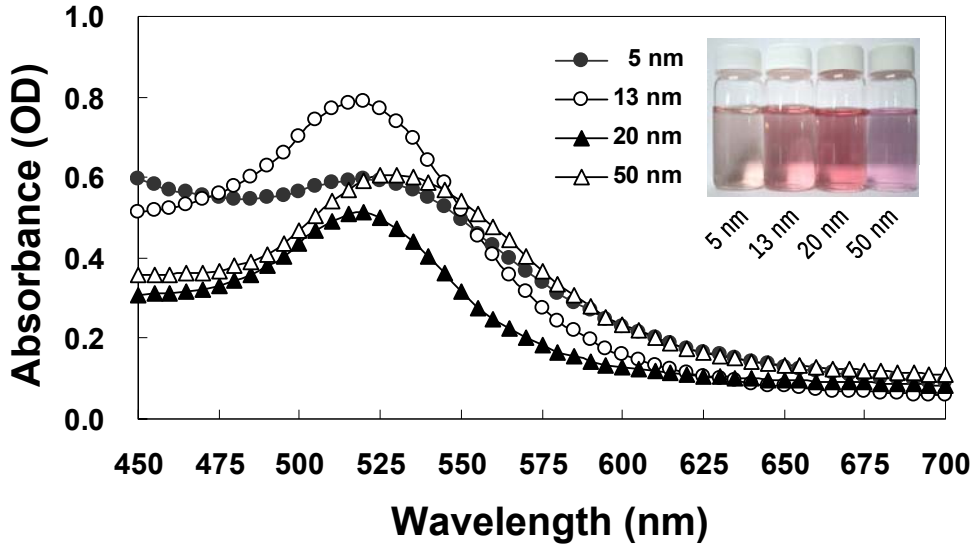

Figure 1-3. UV-Vis absorption spectra of colloidal AuNPs with different diameters. Four sizes of AuNPs (in diameter of 5, 13, 20 and 50 nm) were produced by sodium citrate reduction and the absorption spectra were measured by UV-Vis absorption spectrophotometer. The maximum absorbance (λ_{max}) of the prepared 5, 13, 20 and 50 nm AuNPs were at 515, 520, 524 and 530 nm, respectively. As the size of the AuNPs increases, the surface plasmon band red shifts, resulting in different sizes of AuNPs have exhibited diverse absorption maximum, and display various color.

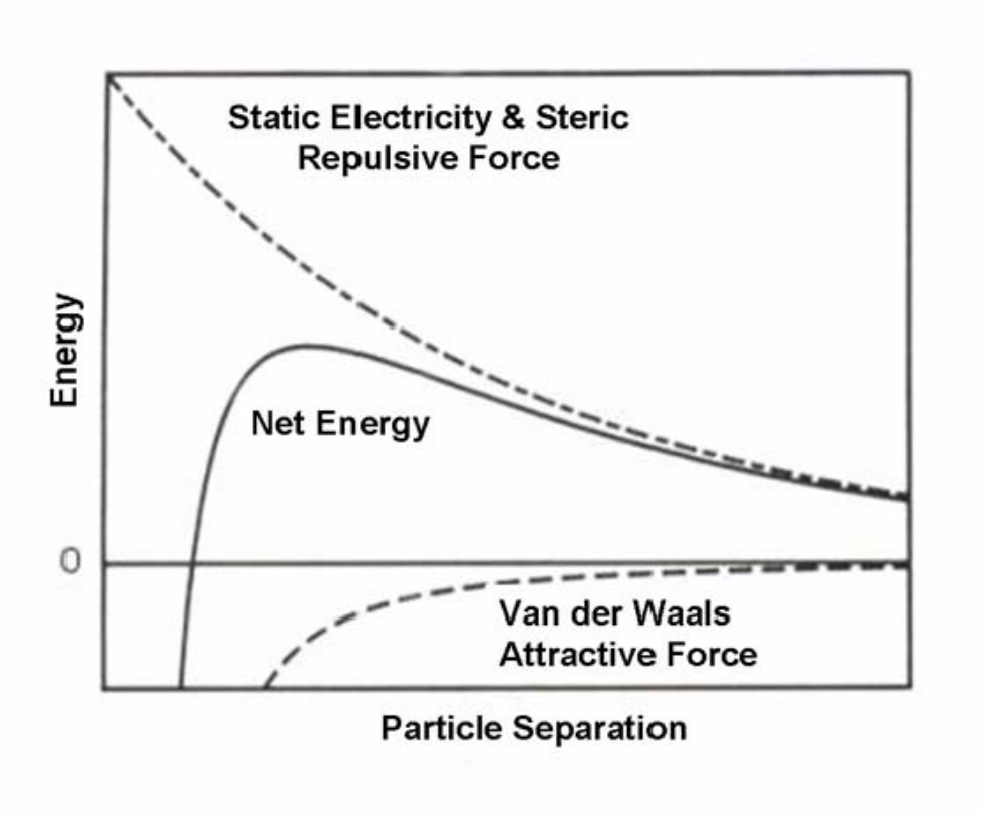

Figure 1-4. The DLVO theory. DLVO theory was developed by Derjaguin and Landau and Verwey and Overbeek in the 1940s, and has been used to explain the stability of colloids in suspension. The theory describes the force between charged surfaces interacting through a liquid medium. The stability of colloidal system is determined by the balance between two opposing forces - electrostatic repulsion and van der Waals attraction.

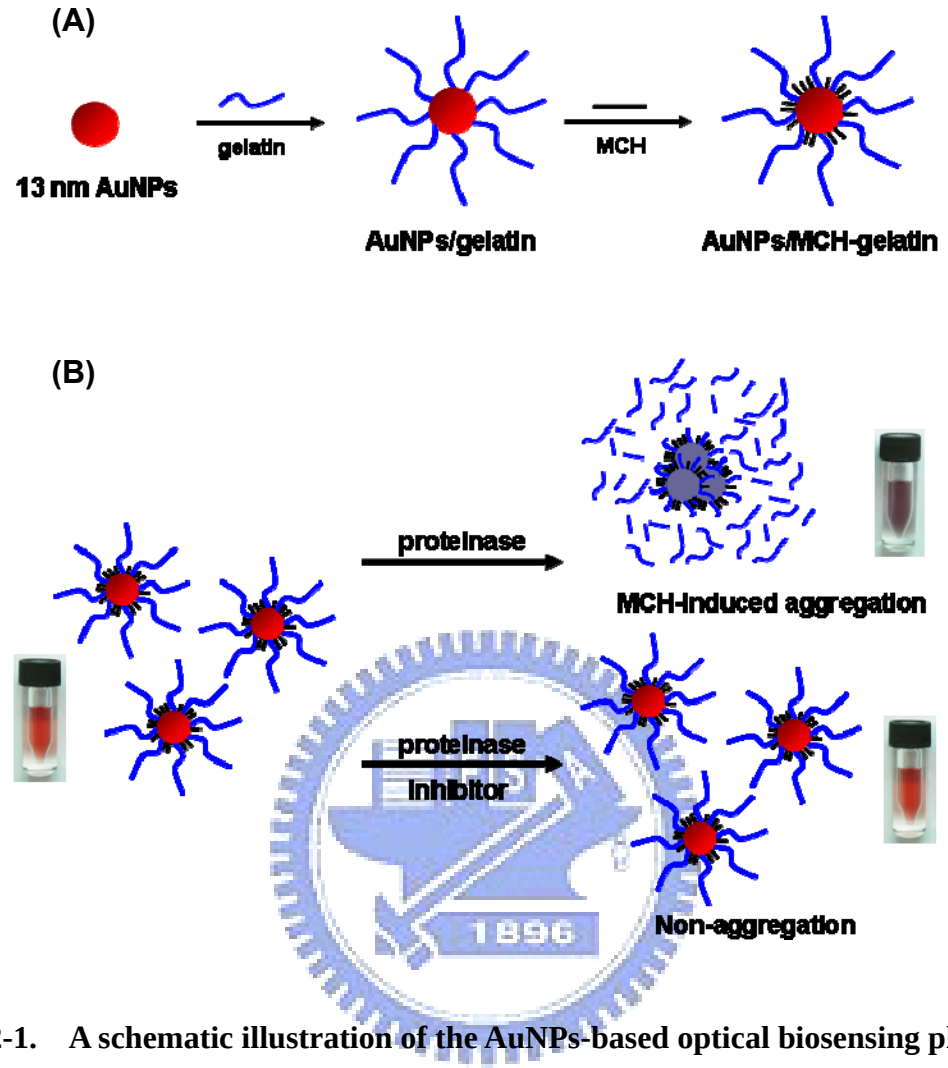

Figure 2-1. A schematic illustration of the AuNPs-based optical biosensing platform to assay proteinase activity. (A) The AuNPs were functionalized with gelatin as proteinase substrate, and modified with MCH as an indicator for the colorimetric detection. (B) When gelatin was digested by proteinase, the AuNPs/gelatin lost shelter to cause aggregation and MCH enhance the attraction among AuNPs. Aggregation of AuNPs would result in a change of color from pink red to violet blue. Besides, when the proteinase activity was blocked by inhibitor, no further color changes in the AuNPs/MCH-gelatin. Therefore, this system can be used to efficient assay proteinase activity and screening the inhibitors of proteinase.

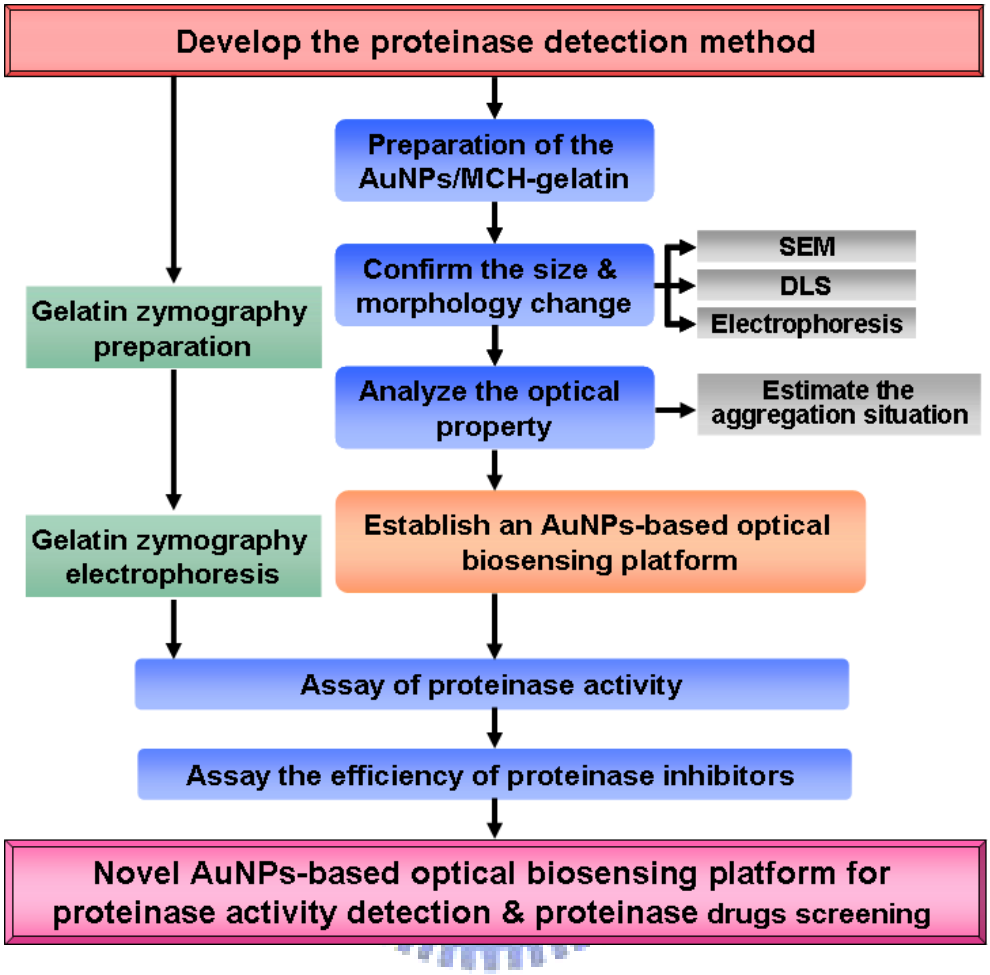

Figure 2-2. The experimental flowchart of study strategies. In this study, 13 nm AuNPs was modified with gelatin and MCH to establish an AuNPs-based optical biosensing platform for assay of proteinase activity and assay the eddiciency of proteinase inhibitors. The characteristic change of AuNPs were investigated by agarose electrophoresis, dynamic light scattering (DLS), scanning electron micrographs (SEM), and UV-Vis absorption spectrum. Finally, this AuNPs-based optical biosensing platform was application in screening the inhibitors of proteinase and detection of proteinase activity.

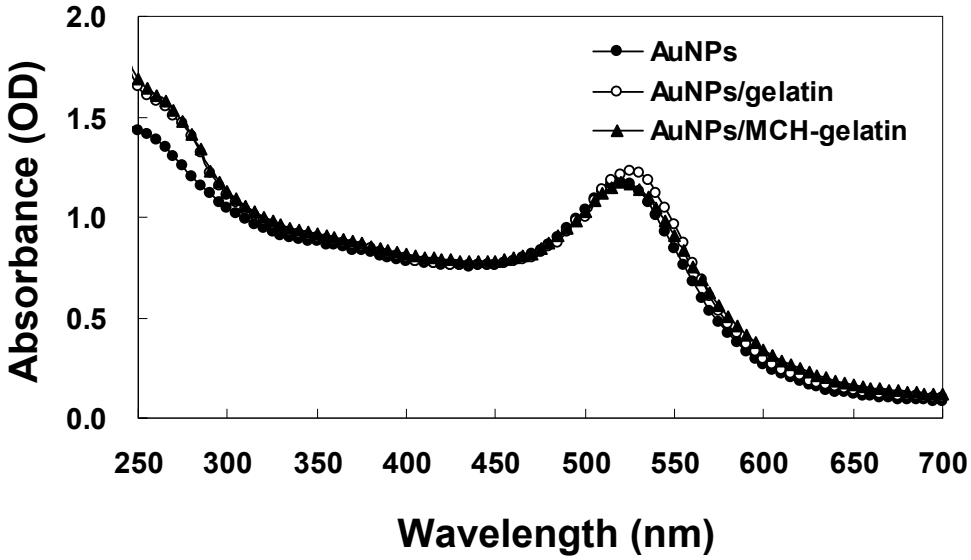

Figure 4-1. UV-Vis absorption spectra of 13 nm AuNPs and modified-AuNPs. The 13 nm AuNPs was prepared by citrate reduction method (●), AuNPs/gelatin (○) was the 13 nm AuNPs modified with 50 mL of 0.1% gelatin, and AuNPs/MCH-gelatin was the 13 nm AuNPs modified with 0.1% gelatin and 1 mM MCH (▲). The λ_{max} of 13 nm AuNPs was located at 520nm. When the 13 nm AuNPs was modified with gelatin, the λmax of modified-AuNPs shifted from 520 to 525 nm, and the peak around 280 nm was due to the absorption by the conjugated gelatin. The diameter of AuNPs/MCH-gelatin did not change remarkably, due to the MCH was a small molecule, and the λ_{max} of gelatin-MCH AuNPs does not shift.

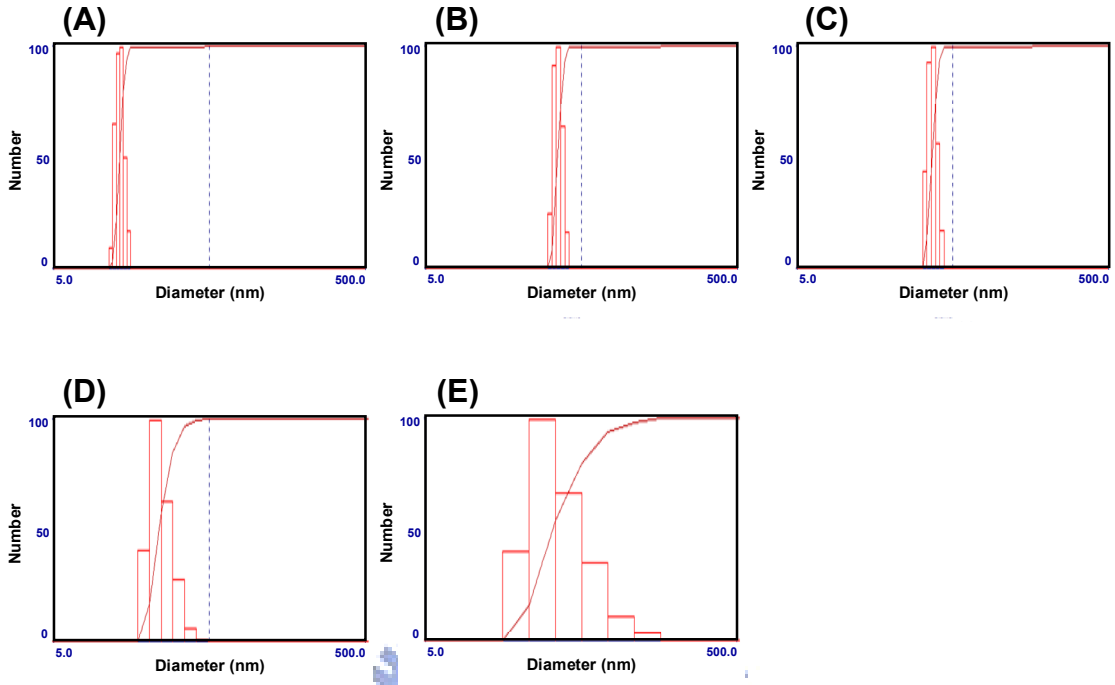

Figure 4-2. The size change of modified-AuNPs. The average particle size of modified-AuNPs were investigated by DLS and analyzed at 20°C. (A) Non-modified AuNPs; The AuNPs/gelatin before (B) and after digested by trypsin (C); The AuNPs/MCH-gelatin (D), and after digested by trypsin (E). X-axis represents the diameter of particles on a logarithm scale. Y-axis represents the relative number of collected particles.

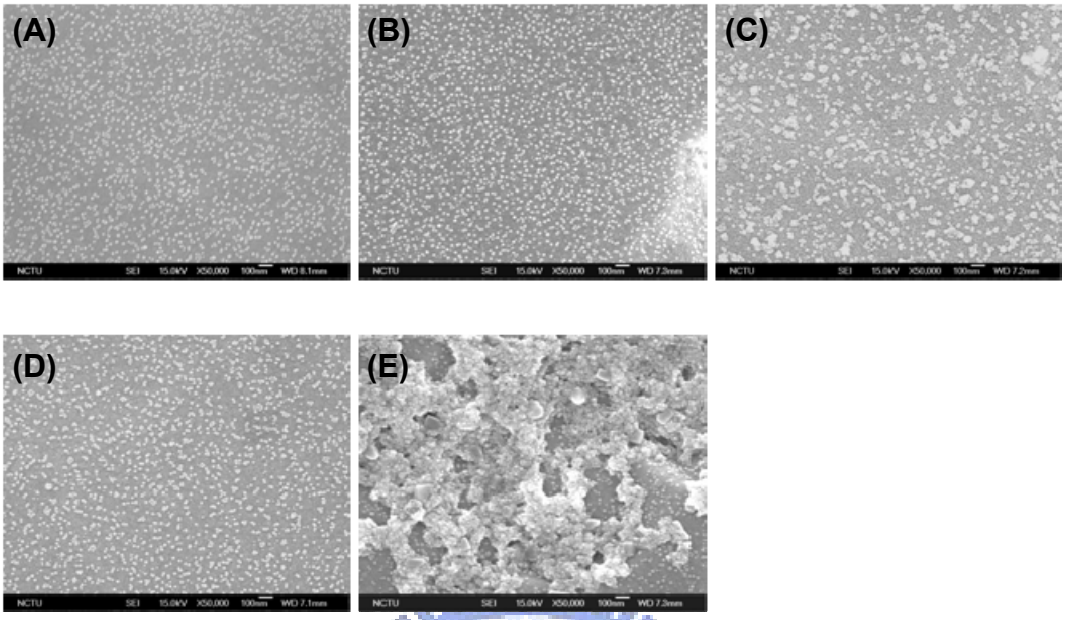

Figure 4-3. Investigating the morphology change of modified-AuNPs. (A) Non-modified AuNPs; The AuNPs/gelatin before (B) and after digested by trypsin (C); The AuNPs/MCHgelatin (D), and after digested by trypsin (E). The non-modified AuNPs was dispersive on the chip due to their negative charge of AuNPs surface would repel each other. (B)(D) The size and morphology of AuNPs/gelatin and AuNPs/MCH-gelatin were similar with each other. After proteinase digested (5×10^{1} U of trypsin), AuNPs/gelatin kept monodispersed (C), however, after proteinase digested AuNPs/MCH-gelatin, MCH induced AuNPs/MCH-gelatin to aggregation (E).

AuNPs	V	V	V	V	V
Gelatin		V	V	V	V
MCH				V	V
Trypsin			V		V

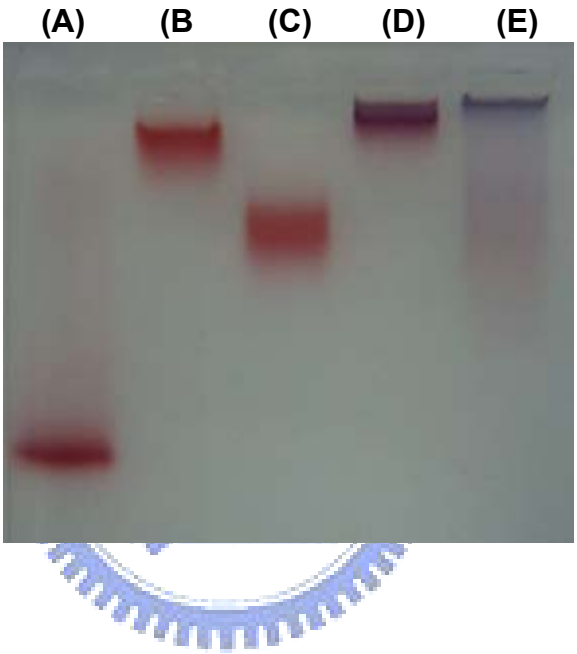

Figure 4-4. The electrophoresis mobility of modified-AuNPs. Electrophoretic separation of modified-AuNPs was according to particles size in 0.5% agarose gel, and run for 30 min at 110 V in 0.5 × TBE buffer. After the modified-AuNPs digested by trypsin, the diameter of AuNPs-gelatin decreased and moved faster than original AuNPs/gelatin; In contrast, most of AuNPs/MCH-gelatin aggregated and remain stay upon gel after digesting by trypsin. (A) Non-modified AuNPs; (B) AuNPs/gelatin; (C) The AuNPs/gelatin after digested by trpsin; (D) AuNPs/MCH-gelatin; (E) The AuNPs/MCH-gelatin after digested by trpsin. The modified-AuNPs were digested by trypsin at 37°C for 10 min.

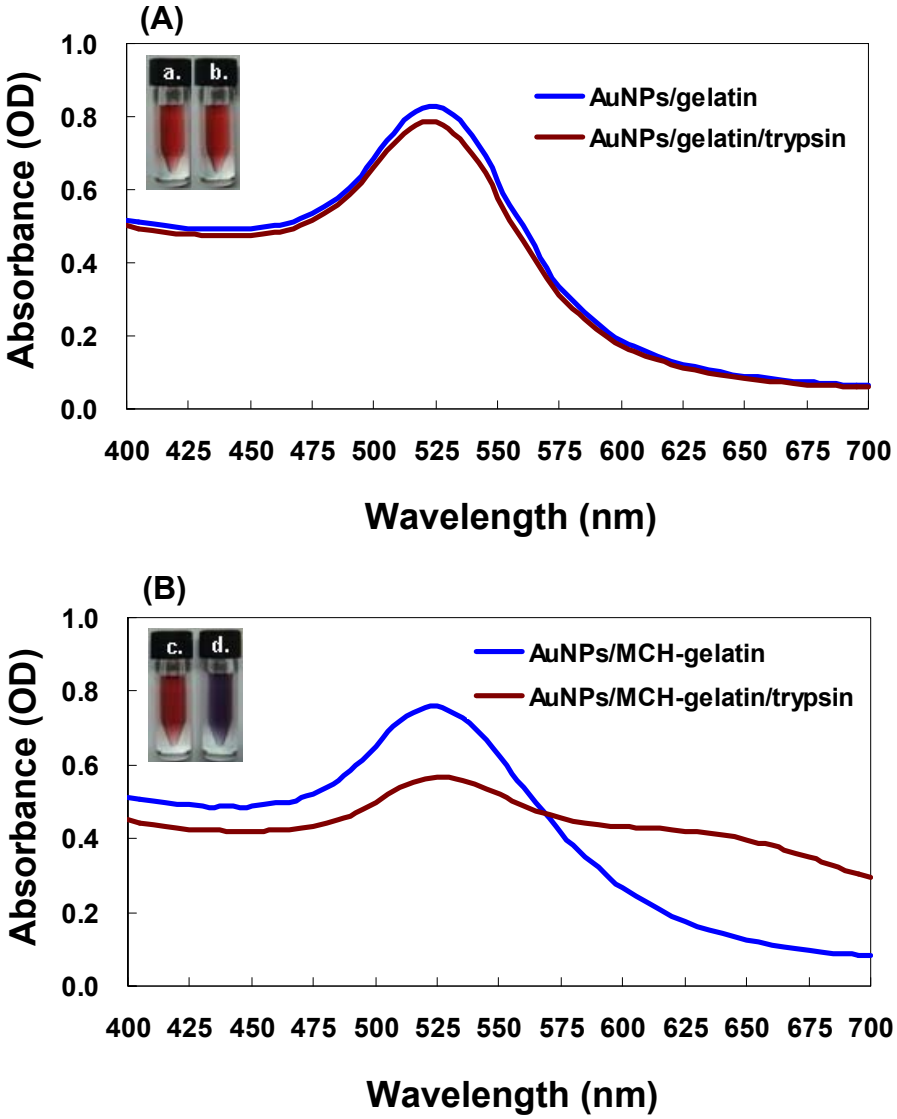

Figure 4-5. The effect of MCH on AuNPs-based optical biosensing platform. (A) Absorbance spectra of AuNPs/gelatin before (blue) and after (red) digeated by proteinase. (B) Similar assay as (A) but used the AuNPs/MCH-gelatin. The inset showed the color change of AuNPs. a, AuNPs/gelatin only; b, AuNPs/gelatin, trypsin; c, AuNPs/MCH-gelatin only; d, AuNPs/MCH-gelatin, trypsin. The modified-AuNPs were digested by 5×10^{1} U proteinase at 37°C for 10 min. The λ_{max} at 525 nm was slightly decrease and without significant red shift in peak position when proteinase was added into AuNPs/gelatin. However, while more proteinase was added into AuNPs/MCH-gelatin, there was not only the absorbance at 525 nm decreased, but also significantly increased absorbance among 600 nm to 650 nm.

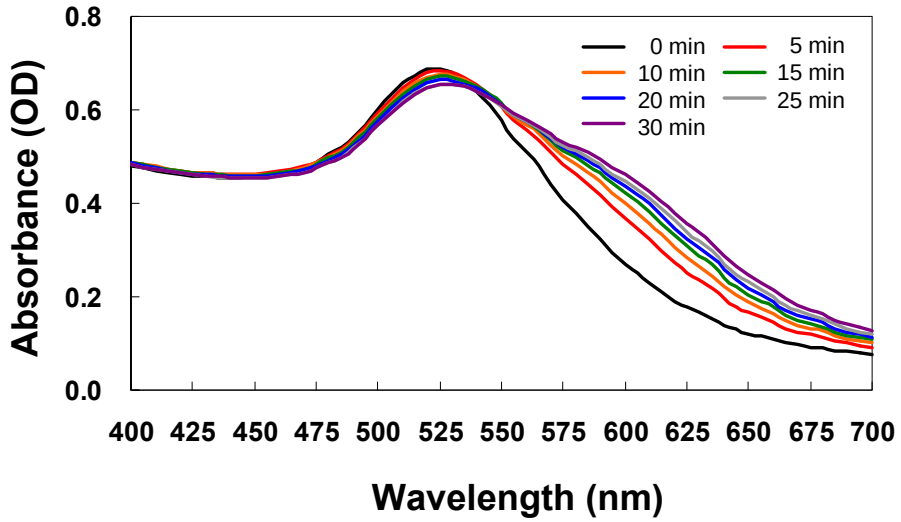

Figure 4-6. Time-dependent changed of absorbance spectrum of AuNPs-based optical biosensing platform. Absorbance spectrum of AuNPs/MCH-gelatin taken at 5 min intervals for 30 min after trypsin digested the substrate. The solution under investigation was composed of 250 mL of AuNPs/MCH-gelatin (5 nM), trypsin (5×10^{1} U). Both a decreased absorbance of the plasmon band at 525 nm and an increased absorbance at 625 nm were observed with increasing time. The new broad absorption at 625 nm emerged was due to the AuNPs/MCH-gelatin began aggregation. For this reason, in this AuNPs-based optical biosensing platform, the absorption ratio ($A_{625\ nm}/A_{525\ nm}$) of AuNPs/MCH-gelatin was used to quantity estimate the proteinase activity.

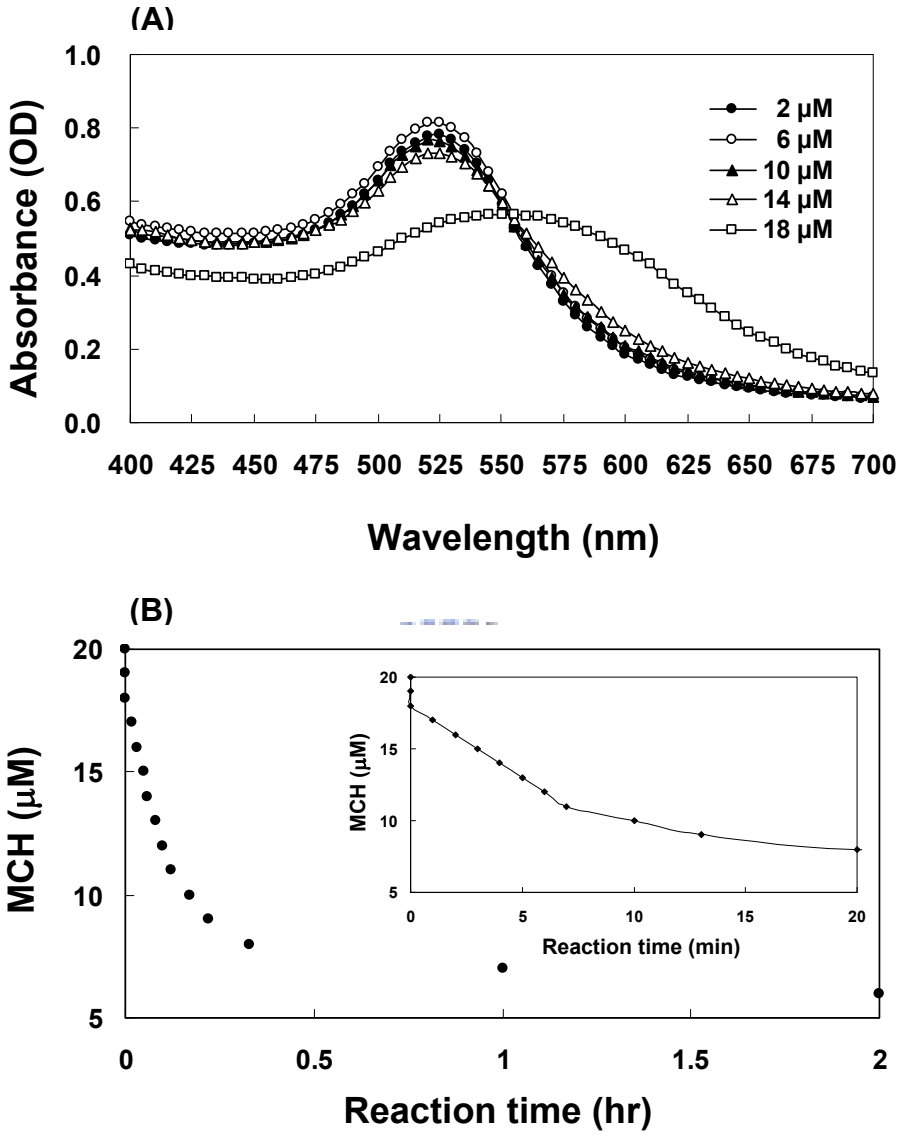

Figure 4-7. The effect of different concentration of MCH on AuNPs-based optical biosensing platform. (A) The spectrum of AuNPs/MCH-gelatin which modified with different concentration of MCH, and response time for AuNPs/MCH-gelatin to aggregate (B). The AuNPs/MCH-gelatin were modified with different concentration of MCH (from 1 to 20 μM), and digested by 5×10^1 U of trypsin.

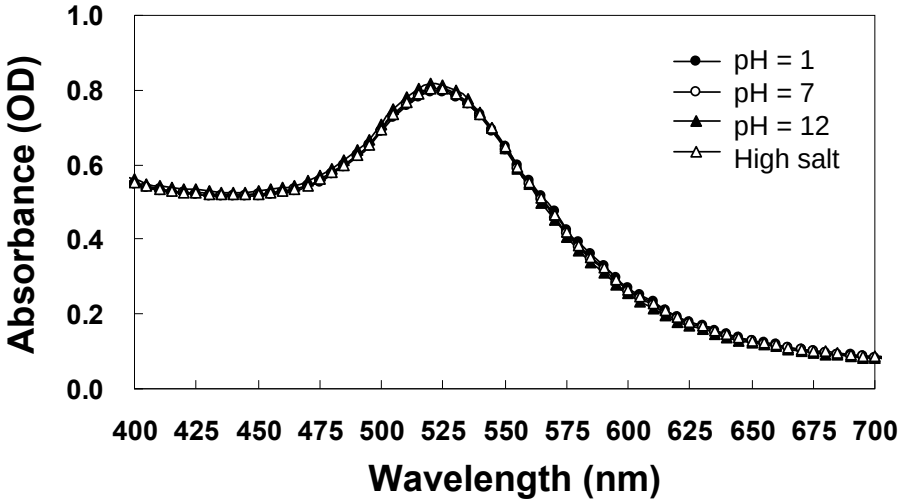

Figure 4-8. The stability of AuNPs/MCH-gelatin in strict environment. The spectra of AuNPs/MCH-gelatin in different buffer solution. The AuNPs/MCH-gelatin in pH 1 (●), pH 7 (○), pH13 (▲), and in high salt buffer (△). The gelatin-MCH AuNPs was protected by substrate, and could stably suspend in strict environment (pH 1, pH 13 or high salt concentration). The λ_{max} of AuNPs/MCH-gelatin and waveform were no change in different buffer condition. Therefore, the AuNPs/MCH-gelatin exhibited a dramatic stability in strict environment.

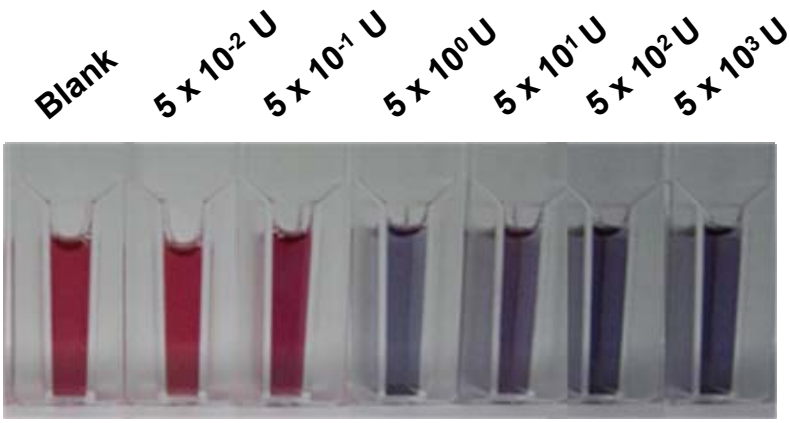

Figure 4-9. Colorimetric assay for trypsin by using AuNPs/MCH-gelatin. The solutions contained AuNPs/MCH-gelatin, and different concentrations of trypsin (from 5×10^{-2} U to 5×10^{3} U). Color changed for the AuNPs/MCH-gelatin solution after the gelatin was hydrolyzed by trypsin at 37°C for 10 min.

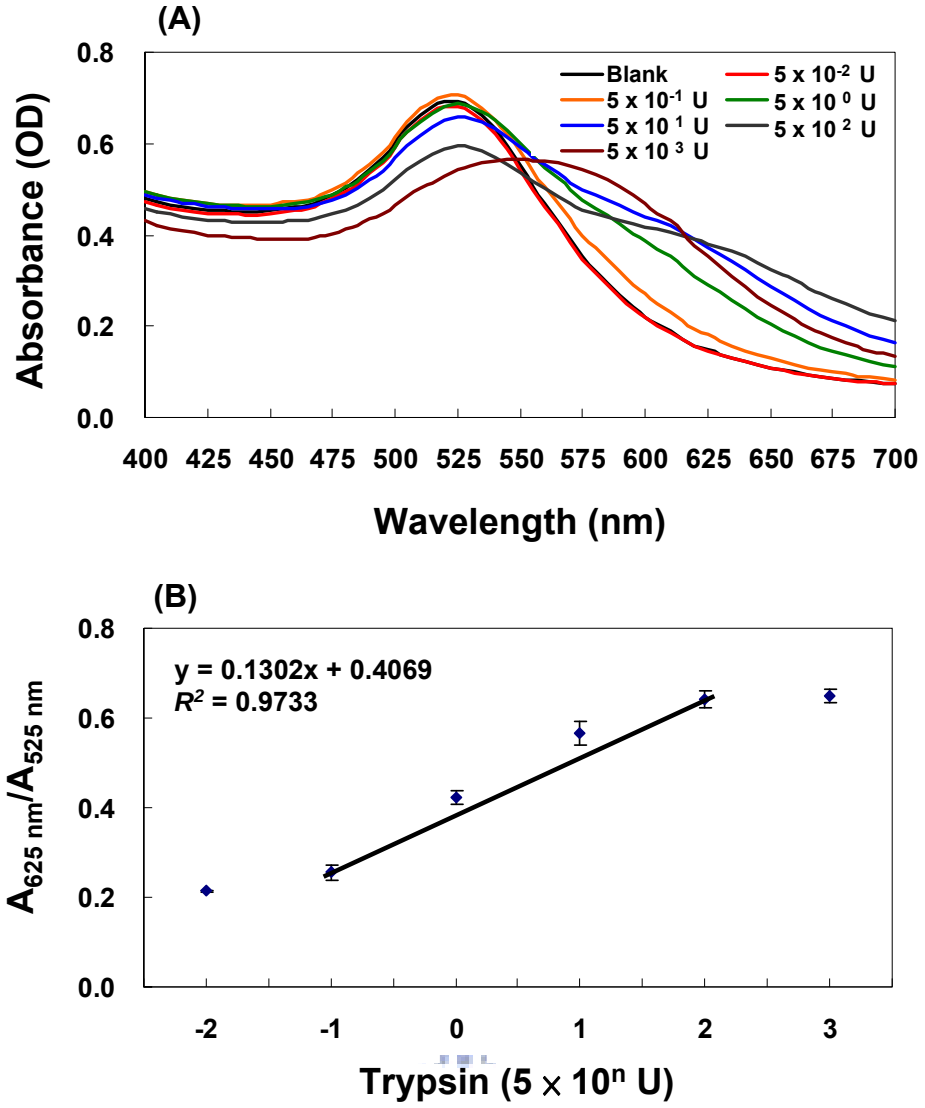

Figure 4-10. Absorption spectra of AuNPs/MCH-gelatin in the presence of trypsin. The solutions contained AuNPs/MCH-gelatin, and different concentrations of trypsin (from 5 × 10^{-2} U to 5 × 10^{3} U). (A) Absorption spectra changed of the AuNPs/MCH-gelatin upon the addition of trypsin; (B) Plot of $A_{625\ nm}/A_{525\ nm}$ of the AuNPs/MCH-gelatin as a function of the trypsin concentration. The samples were incubated at 37°C for 10 min. The linear relationship ranging from 5 × 10^{-1} U to 5 × 10^{2} U of trypsin with regression equation, y = 0.1302x + 0.4096, R^2 = 0.9733. The detection limit is set as signal-to-noise (S/N) = 3, and the detection limit is determined as 5 × 10^{-1} U. Each value was derived from three independent detections and error bars mean standard deviation (SD).

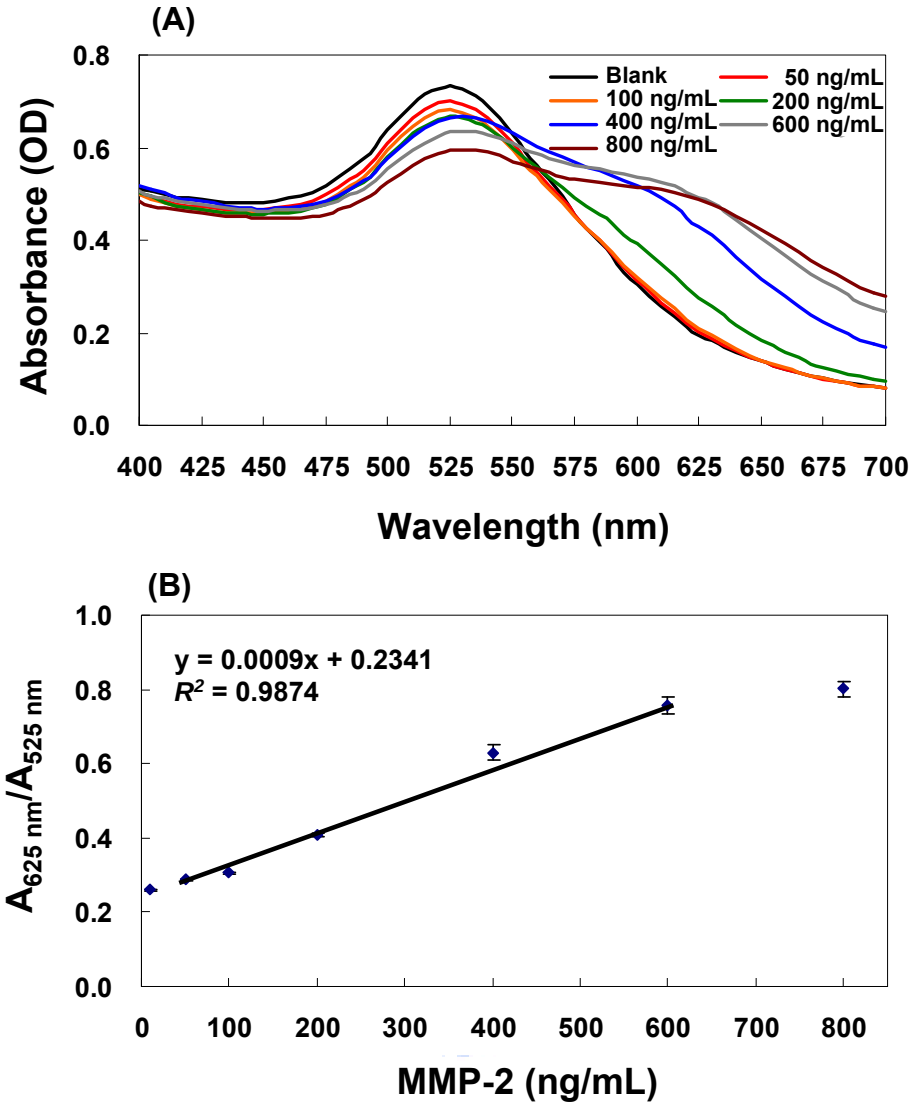

Figure 4-11. Absorption spectra of AuNPs/MCH-gelatin in the presence of MMP-2. The solutions contained AuNPs/MCH-gelatin, and different concentrations of MMP-2 (from 50 ng/mL to 800 ng/mL). (A) Absorption spectra of AuNPs/MCH-gelatin digested by MMP-2. (B) Plot of $A_{625\ nm}/A_{525\ nm}$ of AuNPs/MCH-gelatin against the MMP-2. The samples were incubated at 37°C for 30 min. The linear relationship ranging of the MMP-2 from 50 ng/mL to 600 ng/mL with regression equation, y = 0.0009x + 0.2341, R^2 = 0.9874. The detection limit is set as signal-to-noise (S/N) = 3, and the detection limit is determined as 50 ng/mL. Each value was derived from three independent detections and error bars mean standard deviation (SD).

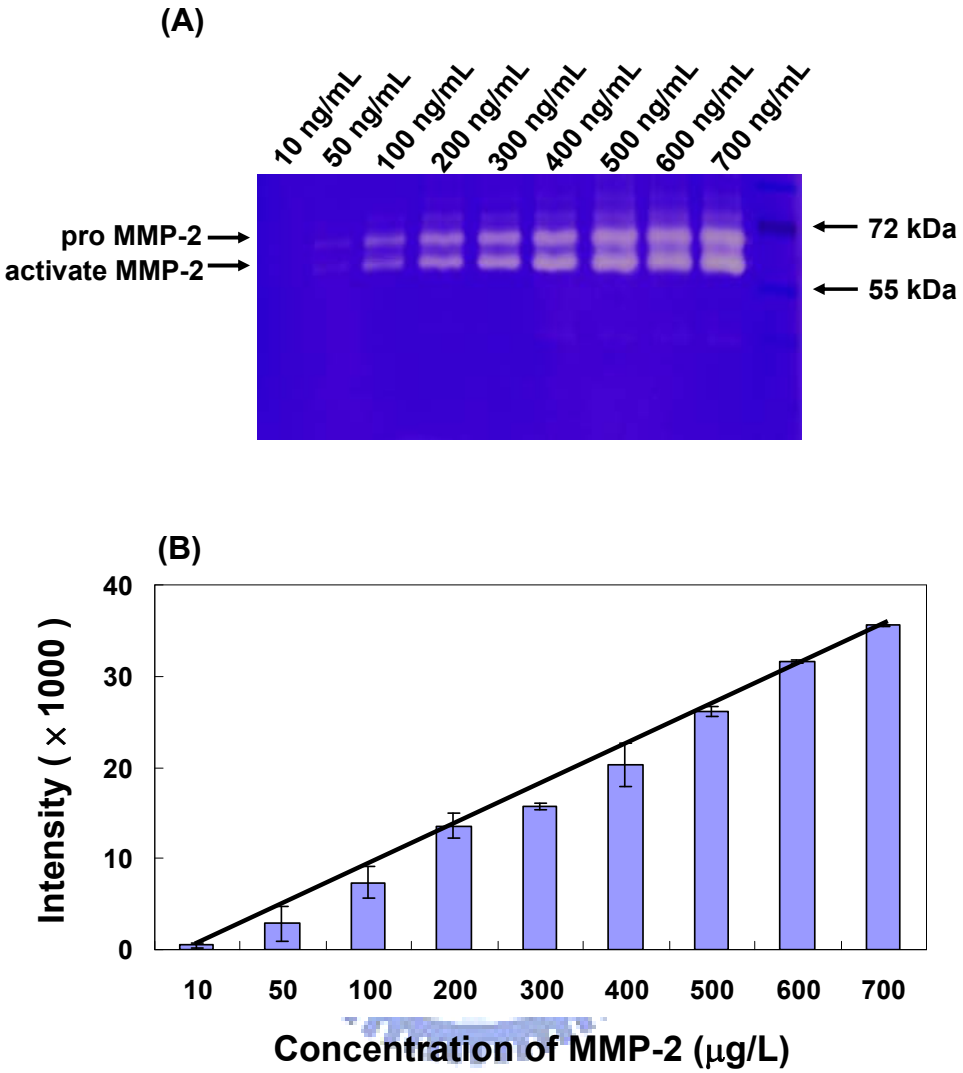

Figure 4-12. Detection of MMP-2 activity by zymography. Zymogram comprised 8% polyacrylamide and 1 mg/mL gelatin. Samples were electrophoresed at constant voltage of 80 V for 4 h. The concentrations of MMP-2 were from 10 ng/mL to 700 ng/mL. (A) The gel of zymography. (B) The gelatinolytic activities of MMP-2. The linear relationship of the MMP-2 was ranged from 10 ng/mL to 700 ng/mL with regression equation, y = 0.0497x + 1.2533, R^2 = 0.9912. The detection limit is set as signal-to-noise (S/N) = 3, and the detection limit is determined as 10 ng/mL.

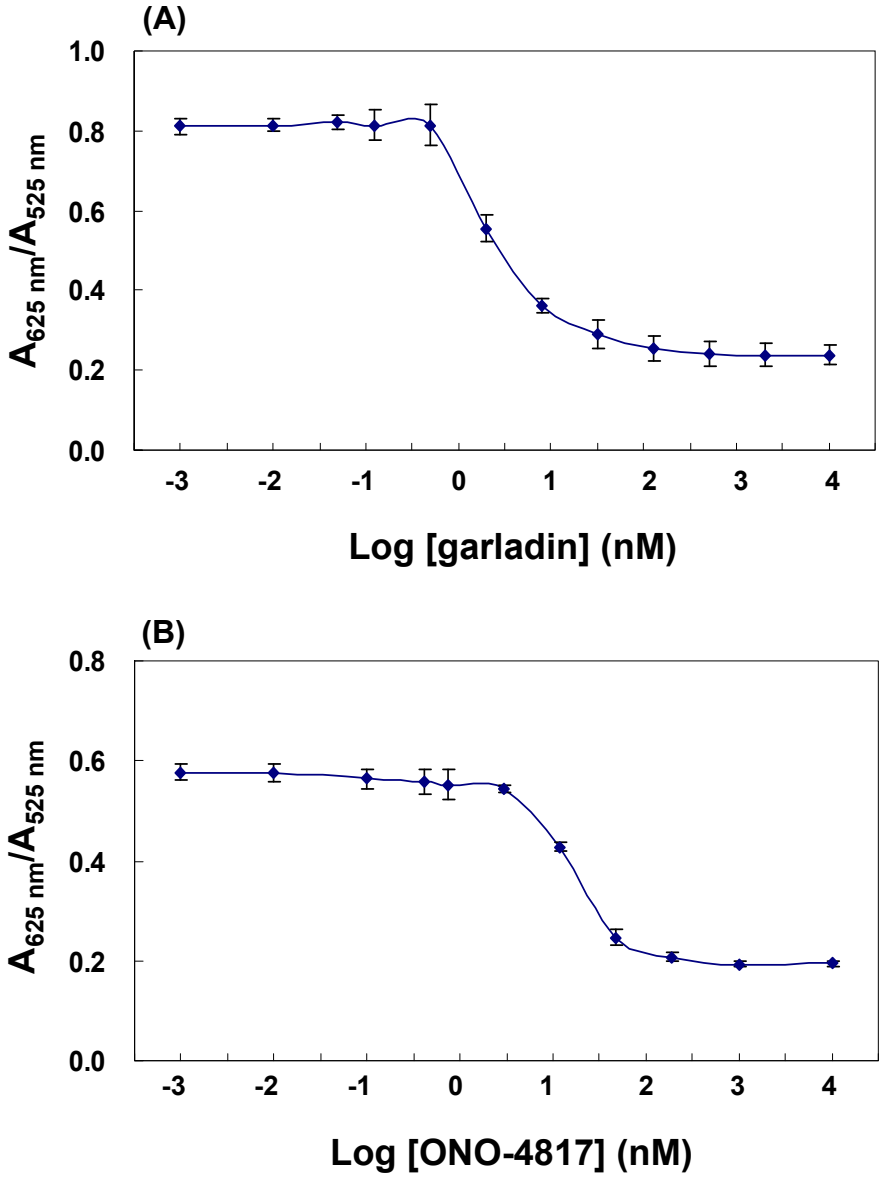

Figure 4-13. Assay the efficiency of MMPs inhibitor by AuNPs-based optical biosensing platform. AuNPs/MCH-gelatin was incubated with MMP-2 and MMP-2 inhibitor at 37°C for 30 min at the same time, then analyzed the $A_{625\ nm}/A_{525\ nm}$ of AuNPs/MCH-gelatin. In the AuNPs-based platform, the galardin (A) and ONO-4817 (B) inhibition with MMPs activity for IC_{50} values were 1.87 nM and 17.76 nM, respectively. Each value was derived from 3 independent detections and error bars mean SD (n = 3).

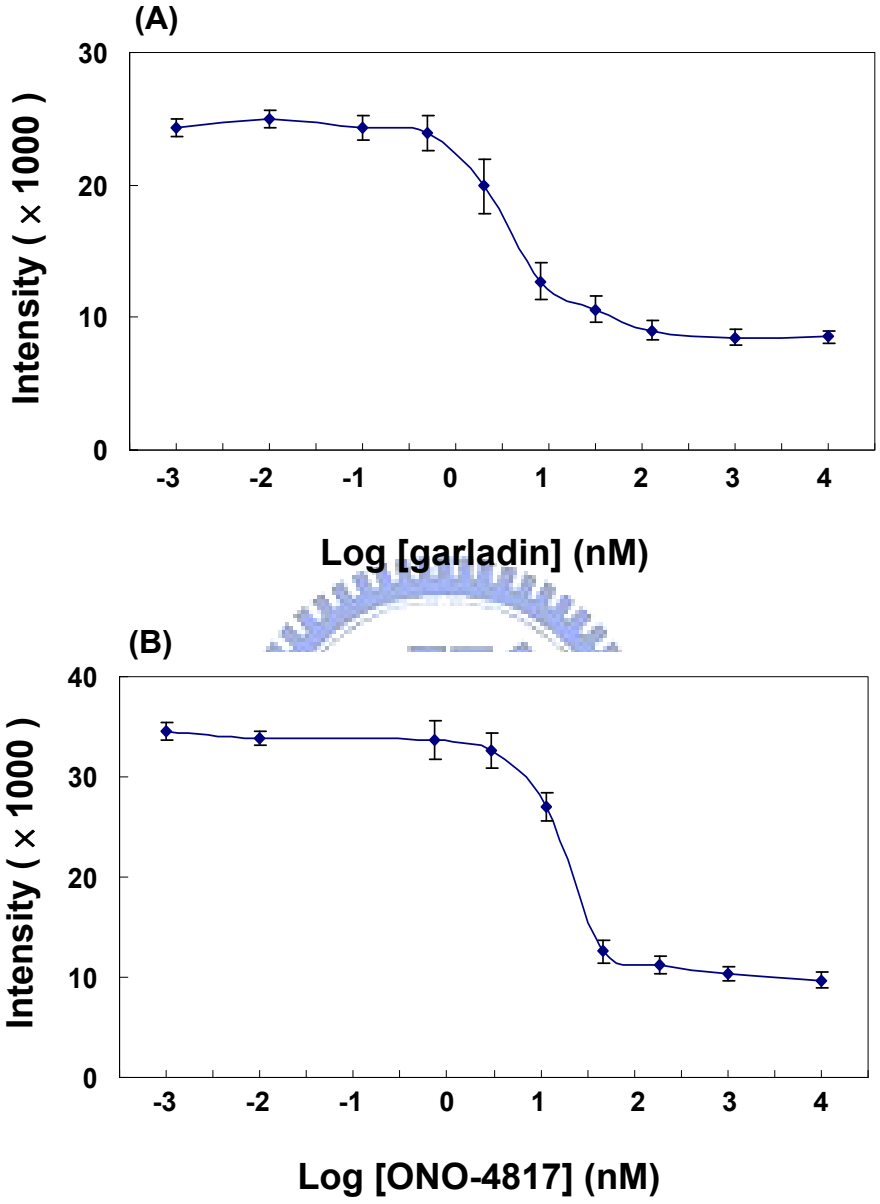

Figure 4-14. Assay the efficiency of MMPs inhibitor by zymography. MMP-2 inhibitor activity was analyzd by 8% gelatin zymography, and gels were incubated with MMP-2 inhibitor at 37°C for 48 hr. The galardin (A) and ONO-4817 (B) inhibition with MMPs activity for IC_{50} values were 3.48 nM and 14.33 nM, respectively.